

RESEARCH ARTICLE

Set-membership estimation of switched LPV systems: Application to fault/disturbance estimation

Shuang Zhang¹  | Vicenç Puig¹  | Sara Ifqir²

¹Institut de Robòtica i informàtica Industrial (CSIC-UPC), Universitat Politècnica de Catalunya-BarcelonaTech, Barcelona, Spain

²CRISTAL, Centrale Lille Institut, Villeneuve d'Ascq, France

Correspondence

Vicenç Puig, Institut de Robòtica i informàtica Industrial (CSIC-UPC), Universitat Politècnica de Catalunya-BarcelonaTech, Carrer Llorens Artigas, 4-6, 08028 Barcelona, Spain.
Email: vicenc.puig@upc.edu

Funding information

European Regional Development Fund, Grant/Award Numbers: 001-P-001643, PID2020-114244RB-I00; DGR of Generalitat de Catalunya, Grant/Award Number: 2017/SGR/482; Chinese Scholarship Council (CSC), Grant/Award Number: 202006120006

Summary

This paper proposes a set-membership state estimation method for Switched Linear Parameter Varying (SLPV) systems subject to unknown but bounded parametric uncertainties, disturbances and noises. A zonotopic outer approximation of the state estimation domain is computed at every time iteration. The size of this zonotope is designed to be convergent and bounded by satisfying P -radius-based and Average Dwell Time (ADT) conditions that are formulated in the Linear Matrix Inequality (LMI) framework. An extension of the state estimation method is presented to address the fault/disturbance estimation problem for SLPV systems. By using the state augmentation technique, the fault/disturbance estimation problem is transformed into a state estimation problem of the generated augmented descriptor switched LPV system. An application to vehicle lateral dynamics fault estimation is used for assessment purposes. Simulation results demonstrate the effectiveness of the proposed algorithm and highlight its advantages over the existing methods.

KEYWORDS

fault/disturbance estimation, set-membership estimation, state estimation, switched LPV systems, zonotopes

1 | INTRODUCTION

In the last decades, state estimation for LPV systems has been widely studied and applied to feedback control^{1,2} and diagnosis.^{3,4} However, when the LPV system operates in a wide operating range and with parameter variations, a single LPV estimator often leads to conservative performance. Since the switched systems are able to describe a wide range of complex and nonlinear behaviours, a reasonable approach to avoid this kind of problem is to use Switched Linear Parameter Varying (SLPV) systems. In this case, the parameter region is divided into smaller subregions such that a series of LPV subsystems are generated. Then, a local LPV estimator can be designed for each LPV subsystem. Theoretically, better performance can be achieved due to the much greater design freedom provided by the switched systems framework. Therefore, SLPV systems have attracted considerable attention for controller design,^{5,6} fault diagnosis⁷ and fault tolerant control.^{8,9}

Switched systems are an important class of hybrid systems, consisting of a family of subsystems and a switching law. Regarding the stability problem of switched systems, important theoretical results have already been achieved using a Common Lyapunov function to guarantee the stability under arbitrary switching,¹⁰ which usually leads to a conservative result. To reduce the conservatism, Multiple Lyapunov functions are proposed for guaranteeing stability under constrained switching with Dwell Time (DT) and Average Dwell Time (ADT).¹¹ Besides, Multiple Fuzzy Lyapunov

functions with ADT concept are employed by Ifqir et al.¹² for stability analysis, with less conservative stability conditions than conventional results.

Meanwhile, great efforts have also been devoted to state estimation and fault diagnosis problems of switched systems, for example, the works of Ethabet et al.,¹³ Ifqir et al.,¹⁴ Du et al.¹⁵ and Li et al.¹⁶ In practice, some uncertainties, such as unknown parameters, process disturbances or measurement noises, are inevitable for most systems. Hence, the state estimation method needs to be robust against these uncertainties. One possibility is to consider set-based state estimation approaches,¹⁷ where the modelling uncertainties are assumed to be unknown but bounded by a priori known bound. In the literature, there are two categories: the one based on the interval observer and the other using a set-membership approach. The interval observer design requires that the estimation error system matrix is Metzler.¹² However, this condition could be very restrictive, especially in the case of a switched interval observer design where the estimation error dynamics should be stable and positive for each subsystem.¹⁴ As an alternative approach, the set-membership state estimation¹⁸ aims to compute a parametrized Feasible Solution Set (FSS) that is consistent with measurement state sets and uncertain state sets. Several types of sets have been proposed to implement set-membership state estimation approaches, such as polytopes,¹⁹ ellipsoids,²⁰ and zonotopes.²¹ As zonotopes provide efficient computation,²² a much more compact representation²³ and can effectively control and mitigate wrapping effect,²⁴ the zonotopic set-membership approach has been widely applied to state estimation²⁵ and fault diagnosis.^{21,26,27}

Regarding the recent studies about the set-membership state estimation problem for switched systems, Fei et al.²⁸ proposed a zonotopic set-membership state estimator for switched systems subject to unknown but bounded disturbances. They adopted P -radius-based criteria for decreasing the size of zonotopic intersection in each iteration and bounding it when subsystems switch. However, the proposed ADT-based criterion leads to conservative estimation results. Ifqir et al.²⁹ proposed a new P -radius based criterion, which is proven to be a less complex solution with less conservative performance, to reduce the size of the zonotopic intersection at each sample time. However, this work did not consider the ADT switching when designing the switched estimator. For SLPV systems, state estimation design has been implemented by interval observer, parameter identification and adaptive observer, for example, the works of Ifqir et al.,¹² Rios et al.³⁰ and Rotondo et al.³¹ To the best of our knowledge, no research related to the set-membership estimation for SLPV systems can be found.

Fault estimation is a significant stage of fault diagnosis and an essential part for active fault tolerant control. In the literature, there are two families of fault estimation approaches: one regards the fault vector as an unknown input,³² and the other treats the fault vector as an auxiliary state by means of an augmentation technique.^{33,34} Regarding the second family, with the aid of the augmentation technique, the nominal system can be rewritten as an augmented system. Then, the fault estimation problem is transformed into a state estimation problem. Therefore, most existing state estimation approaches can be promoted to fault estimation using this approach. Due to its convenience and effectiveness in estimating the fault vector, quite a lot of results using the augmentation technique performing fault estimation have been published for LTI systems,³⁴ LPV systems,^{33,35} Takagi-Sugeno fuzzy systems.^{36,37} In particular, Zhou et al.³⁵ proposed a zonotopic set-membership estimator of LPV systems for actuator and sensor faults estimation and used a conventional online F -norm based method to obtain the observer gain. As we know, such online observer gain is obtained by minimizing F -norm at each instant, thus, convergence of the estimation is not guaranteed. Besides, the considered actuator and sensor faults in this work are performed using the same fault vector, which is usually rare in real situations.

Inspired by the aforementioned discussions, the aim of this paper is to propose a zonotopic set-membership state estimation method for discrete-time SLPV systems for the first time, and extend this state estimation method to fault/disturbance estimation with the augmentation technique, as depicted by Figure 1. Moreover, unknown but bounded parametric uncertainty, disturbance and noises are considered. The estimator correction matrix design is formulated as an optimization problem in terms of Linear Matrix Inequalities (LMIs) using a less conservative mode-dependent P -radius minimization criterion and ADT switching constraint. The objective is to find admissible switching signals such that the designed estimator is convergent and stable.

The main contributions of this paper are as follows: (1) This paper develops the set-membership state estimation for SLPV systems subject to unmeasurable but bounded scheduling parameters, and bounded disturbance and noises. (2) Compared with the earlier work,²⁸ less conservative P -radius based criteria with ADT switching are proposed for the convergence and stability of the state estimator. (3) By considering the fault/disturbance vector as an auxiliary state, the proposed state estimation method can be further applied to actuator/sensor fault estimation or input disturbance estimation, which provides a broader application scope. (4) Different from the work,³⁵ this paper offers an offline P -radius based approach to compute the correction matrix, which could additionally guarantee the convergence of the estimator.

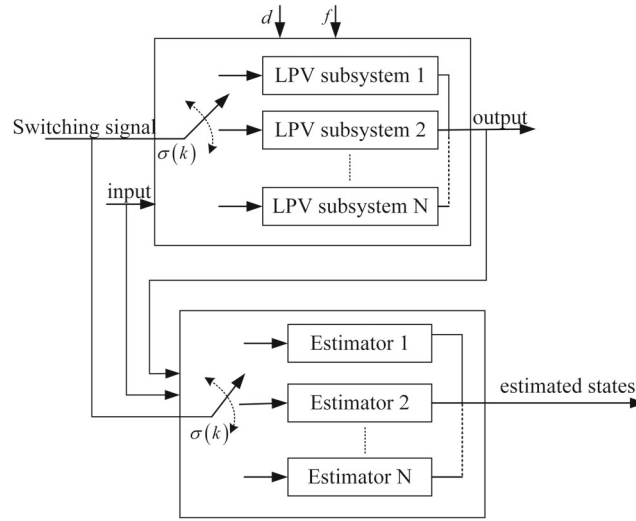


FIGURE 1 Structure of state estimation for SLPV systems.

This paper is organized as: Some preliminary results including definitions, properties and lemmas that will be used in this paper are addressed in Section 2. The problem statement is formulated in Section 3. In Section 4, the details of state estimation for SLPV systems including set-membership state estimation design and optimal switched polytopic correction matrix computation are presented. Section 5 presents the extension of the proposed estimation method to fault/disturbance estimation by using an augmented descriptor SLPV systems. Section 6 illustrates the effectiveness of the proposed method through an application to vehicle lateral dynamics state and fault estimation. Finally, some conclusions are drawn in Section 7.

Notation: In the following, \mathbb{R}^n denotes the set of n -dimensional real numbers and \oplus denotes the Minkowski sum. The matrices are written using capital letter, for example, A , the calligraphic notation is used for denoting sets, for example, \mathcal{X} , the interval matrices are denoted by capital letter with square brackets, for example, $[A]$, $[\underline{x}, \bar{x}]$ is an interval with lower bound \underline{x} and upper bound \bar{x} . For $s \in \mathbb{R}^n$, $\|s\|$ denotes Euclidean vector norm, $\|s\|_p = \sqrt{s^T P s}$ denotes weighted Euclidean vector norm, where $P > 0$. For simplification, the time instant $k + 1$, $k - 1$ is presented by $+$, $-$, respectively, i.e., $x(k + 1) = x(+)$, $x(k - 1) = x(-)$.

2 | PRELIMINARIES

Definition 1. A unitary interval is a vector denoted by $\mathbf{B} = [-1, 1]$. A unitary box in \mathbb{R}^m , denoted by \mathbf{B}^m , is a box composed of m unitary intervals. Given a box $M = ([a_1, b_1], \dots, [a_n, b_n])^T$, $\text{mid}(M)$ denotes its center and $\text{diam}(M) = (b_1 - a_1, \dots, b_n - a_n)^T$.

Definition 2 (Zonotope³⁸). A zonotope of order m in \mathbb{R}^n is the translation by the center $c \in \mathbb{R}^n$ of the image of an unitary hypercube of dimension m in \mathbb{R}^n under a linear transformation $R \in \mathbb{R}^{n \times m}$, the zonotope \mathcal{X} is defined by:

$$\mathcal{X} = \langle c, R \rangle = c \oplus R\mathbf{B}^m = \{p + Rz : z \in \mathbf{B}^m\}$$

Besides, the following properties related to zonotopes hold:

$$\begin{aligned} \langle c_1, R_1 \rangle \oplus \langle c_2, R_2 \rangle &= \langle c_1 + c_2, [R_1, R_2] \rangle, \\ L \odot \langle c, R \rangle &= \langle Lc, LR \rangle, \end{aligned}$$

where L is an arbitrary matrix of appropriate dimension.

Definition 3 (P -radius³⁸). Given a zonotope $\mathcal{X} = \langle c, R \rangle \subset \mathbb{R}^n$ of order m and a weighting matrix $P = P^T > 0$, the P -radius of \mathcal{X} is defined by

$$l = \max_{x \in \mathcal{X}} \|x - c\|_P^2 = \max_{z \in \mathbf{B}^m} \|Rz\|_P^2$$

Definition 4 (ADT³⁹). For a switching signal $\sigma(k)$ and any time instant $K > k > 0$, let $N_\sigma(k, K)$ denote the switching times of σ during the interval $[k, K]$. If for any given $N_0 > 0$ and $\tau_a > 0$, we have

$$N_\sigma(k, K) \leq N_0 + \frac{K - k}{\tau_a}, \forall K \geq k \geq 0,$$

then N_0 and τ_a are called the chatter bound and the Average Dwell Time (ADT) respectively. We can set $N_0 = 0$ as commonly used in the literature.

Property 1 (Zonotope inclusion¹⁸). Consider a family of zonotopes represented by $\mathcal{X} = c \oplus [M]\mathbf{B}^m$, where $c \in \mathbb{R}^n$ is a real vector and $[M] \in \mathbb{R}^{n \times m}$ is an interval matrix. A zonotope inclusion, denoted by $\diamond(Z)$, is defined by

$$\diamond(Z) = p \oplus [\text{mid}([M]) \quad \text{rs}(\text{diam}([M])/2)] \begin{bmatrix} \mathbf{B}^m \\ \mathbf{B}^n \end{bmatrix}$$

where $\text{rs}(\text{diam}([M])/2)$ is a diagonal matrix with diagonal elements $\text{rs}(\text{diam}([M])/2)_{ii} = \sum_{j=1}^m |\text{diam}([M])/2_{ij}|$, $i = 1, 2, \dots, n$. Under these definitions, $Z \subseteq \diamond(Z)$.

Property 2 (State zonotope inclusion⁴⁰). Given a state-space model $x(k+1) = Ax(k) + Bu(k)$, $x(k) \in \mathbb{R}^{n_x}$ is the state vector, $u(k) \in \mathbb{R}^{n_u}$ is the input vector, $A \in \mathbb{R}^{n_x \times n_x}$ and $B \in \mathbb{R}^{n_x \times n_u}$ are the uncertain state-space matrices belonging to the interval matrices $[A]$ and $[B]$, respectively. Considering $x(k) \in \mathcal{X}_k = \langle c_k, R_k \rangle$, the state $x(k+1)$ is bounded by a zonotope $\mathcal{X}_{k+1} = \langle c_{k+1}, R_{k+1} \rangle$ represented as

$$\begin{aligned} c_{k+1} &= \text{mid}([A])c_{x,k} + \text{mid}([B])u_k, \\ R_{k+1} &= \left[\text{seg}(\diamond([A]R_k)) \quad \frac{\text{diam}([A])}{2}c_k \quad \frac{\text{diam}([B])}{2}u_k \right] \end{aligned}$$

where $\text{seg}(\diamond([A]R_k))$ means computing the zonotope segment matrix with Property 1.

Property 3. Given an interval matrix $[A] \in \mathbb{R}^{n \times p}$ and a real matrix $B \in \mathbb{R}^{p \times q}$, the center and the diameter of their product $[A]B$ are

$$\begin{aligned} \text{mid}([A]B) &= (\text{mid}[A])B \\ \text{diam}([A]B) &= (\text{diam}[A])|B| \end{aligned}$$

where each element of $|B|$ is formed with the absolute value of its corresponding element of B .⁴¹

Property 4. If M is positive semidefinite, then $A^T M A$ is positive semidefinite for any (possibly rectangular) matrix A . If M is positive definite and A has full column rank, then $A^T M A$ is positive definite.

Property 5 (Zonotope intersection¹⁸). Given the zonotope $\mathcal{X} = \langle c_x, R_x \rangle \in \mathbb{R}^n$, the strip $\mathcal{X}_y = \{x \in \mathbb{R}^n : |Cx - d| \leq \sigma\}$ and the vector $\lambda \in \mathbb{R}^n$, the intersection between the zonotope and the strip is defined as $\mathcal{X} \cap \mathcal{X}_y = \langle c, R \rangle$, where $c = c_x + \lambda(d - Cc_x)$ and $R = [(I - \lambda C)R_x \quad \sigma\lambda]$.

Property 6 (Zonotope reduction⁴²). A reduction operator, denoted $\downarrow_{q,W}$, allows to reduce the number of generators of a zonotope \mathcal{X} to a fixed number $n \leq q < m$, such that $\mathcal{X} = \langle c, R \rangle \subset \langle p, \downarrow_{q,W} R \rangle$. A common procedure for implementing the operator $\downarrow_{q,W}$ is summarized as follows: Sort the column of segment matrix $R \in \mathbb{R}^{n \times m}$ in decreasing weighted vector norm $\|\cdot\|_W$, $R = [r_1, \dots, r_j, \dots, r_m]$, $\|r_j\|_W^2 \geq \|r_{j+1}\|_W^2$; Enclose the set $R_{>}$ generated by the $m - q + n$ smaller columns into a box (i.e., interval hull):

If $m \leq q$, then $\downarrow_{q,W} R = R$, Else

$$\downarrow_{q,W} R = [R_{>}, \text{rs}(R_{<})] \in \mathbb{R}^{n \times q}, R_{>} = [r_1, \dots, r_{q-n}], R_{<} = [r_{q-n+1}, \dots, r_m]$$

where $r(R_{<})$ is a diagonal matrix with diagonal elements of $\text{rs}(R_{<})_{i,i} = \sum_{j=1}^m |R_{<}|_{ij}$, $i = 1, \dots, n$.

Lemma 1 ⁽⁴³⁾. Given matrices $X \in \mathbb{R}^{a \times b}$, $Y \in \mathbb{R}^{b \times c}$ and $Z \in \mathbb{R}^{a \times c}$, if $\text{rank}(Y) = c$, then the general solution of the $XY = Z$ is

$$X = ZY^\dagger + R(I_b - YY^\dagger)$$

where $Y^\dagger = Y^T(YY^T)^{-1}$ is the Moore-Penrose inverse of matrix Y , $R \in \mathbb{R}^{a \times b}$ is an arbitrary matrix.

3 | PROBLEM STATEMENT

Consider the following switched discrete-time LPV system subject to parameter uncertainties and noises

$$\begin{cases} x(+) = A_{\sigma(k)}(\rho(k), \xi(k))x(k) + B_{\sigma(k)}(\rho(k), \xi(k))u(k) + E_w w(k) \\ y(k) = Cx(k) + E_v v(k) \end{cases}, \quad (1)$$

where $x \in \mathbb{R}^{n_x}$ is the state, $u \in \mathbb{R}^{n_u}$ is the control input, $y \in \mathbb{R}^{n_y}$ is the measured output. $\sigma(k) : \mathbb{R}^+ \rightarrow \mathcal{I} = \{1, 2, \dots, I\}$ is a known switching signal, satisfying the ADT switching scheme,⁴⁴ assumed to be online available, where I denotes the number of subsystems. We employ a sequence $k_1, k_2, \dots, k_l, k_{l+1}, \dots, k_{N_\sigma(k_0, K)}$ to represent the switching instants on the interval $[k_0, K)$, where $k_0 = 0$ denotes the initial time, k_l denotes the l^{th} switching instant and the active i^{th} subsystem ($\sigma(k) = i$) when $k \in [k_l, k_{l+1})$. $A_{\sigma(k)}(\rho(k), \xi(k)) \in \mathbb{R}^{n_x \times n_x}$ and $B_{\sigma(k)}(\rho(k), \xi(k)) \in \mathbb{R}^{n_x \times n_u}$ are unknown parametric matrices depending respectively on the measurable and unmeasurable scheduling vectors $\rho \in \mathbb{R}^{n_r}$ and $\xi \in \mathbb{R}^{n_s}$. $E_w \in \mathbb{R}^{n_x \times n_w}$, $E_v \in \mathbb{R}^{n_y \times n_v}$ and $C \in \mathbb{R}^{n_y \times n_x}$ are constant matrices. $w(k) \in \mathbb{R}^{n_w}$ and $v(k) \in \mathbb{R}^{n_v}$ are the process and measurement noises, respectively, assumed to be unknown but bounded by zonotopes, that is, $w(k) \in \mathcal{W} = \langle 0, I_{n_w} \rangle$, $v(k) \in \mathcal{V} = \langle 0, I_{n_v} \rangle$, where $I_{n_w} \in \mathbb{R}^{n_w \times n_w}$ and $I_{n_v} \in \mathbb{R}^{n_v \times n_v}$ denote the identity matrices. It is assumed that the unknown scheduling vector $\xi(k)$ is composed by a priori known constant nominal value ξ_0 which is affected by an unknown uncertainty $\Delta\xi(k)$ such that

$$\xi(k) = \xi_0 + \Delta\xi(k). \quad (2)$$

Therefore, the state matrices can be written as a nominal part plus an uncertain part based on (2) as:

$$\begin{aligned} A_{\sigma(k)}(\rho(k), \xi(k)) &= A_{\sigma(k)}(\rho(k), \xi_0) + \Delta A_{\sigma(k)}(\rho(k), \Delta\xi(k)), \\ B_{\sigma(k)}(\rho(k), \xi(k)) &= B_{\sigma(k)}(\rho(k), \xi_0) + \Delta B_{\sigma(k)}(\rho(k), \Delta\xi(k)), \end{aligned} \quad (3)$$

For simplification, we denote the nominal part $A_{\sigma(k)}(\rho(k), \xi_0)$ and $B_{\sigma(k)}(\rho(k), \xi_0)$ by $A_{\sigma(k)}(\rho(k))$ and $B_{\sigma(k)}(\rho(k))$, respectively. According to Reference 45, the uncertainties on system matrices caused by the uncertain parameter $\xi(k)$ can be approximated by an uncertain term $E_{\theta, \sigma(k)}(\rho(k))\theta(k)$ as in (4),

$$\Delta A_{\sigma(k)}(\rho(k), \Delta\xi(k))x(k) + \Delta B_{\sigma(k)}(\rho(k), \Delta\xi(k))u(k) \approx E_{\theta, \sigma(k)}(\rho(k))\theta(k), \theta(k) \in [-1, 1]^{n_\theta} = \langle 0, I_{n_\theta} \rangle, \quad (4)$$

where $\theta(k)$ is an unknown but constant vector that represents the parametric uncertainty, and $E_{\theta, \sigma(k)}(\rho(k))$ is the associated non-empty distribution matrix of suitable dimensions that models the direction and scale of the parametric uncertainty.

In the sequel, the system (1) can be rewritten as:

$$\begin{cases} x(+) = A_{\sigma(k)}(\rho(k))x(k) + B_{\sigma(k)}(\rho(k))u(k) + E_{\theta, \sigma(k)}(\rho(k))\theta(k) + E_w w(k) \\ y(k) = Cx(k) + E_v v(k) \end{cases} \quad (5)$$

Furthermore, considering that variable $\rho(k)$ is online measurable and setting it as the scheduling variable leads to the following polytopic form of system (5):

$$\begin{cases} x(+) = \sum_{j=1}^J h_{\sigma(k)}^j(\rho(k)) \left(A_{\sigma(k)}^j x(k) + B_{\sigma(k)}^j u(k) + E_{\theta, \sigma(k)}^j \theta(k) \right) + E_w w(k) \\ y(k) = Cx(k) + E_v v(k) \end{cases} \quad (6)$$

with

$$\Delta A_{\sigma(k)}^j(\Delta\xi)x(k) + \Delta B_{\sigma(k)}^j(\Delta\xi)u(k) \approx E_{\theta,\sigma(k)}^j \theta(k) \quad (7)$$

where $A_{\sigma(k)}^j$, $B_{\sigma(k)}^j$, and $E_{\theta,\sigma(k)}^j$ for $j = 1, \dots, J$ are known constant matrices and $h_{\sigma(k)}^j(\rho(k))$ are the weighting function for the j^{th} sub-model depending on the time varying parameter $\rho(k)$ that fulfills the following properties

$$\sum_{j=1}^J h_{\sigma(k)}^j(\rho(k)) = 1, \quad 0 \leq h_{\sigma(k)}^j(\rho(k)) \leq 1, \quad \forall j = \{1, \dots, J\} \quad (8)$$

In order to bound the mode-dependent uncertainty term $\Delta A_{\sigma(k)}^j(\Delta\xi)x(k) + \Delta B_{\sigma(k)}^j(\Delta\xi)u(k)$, the uncertain system matrices are denoted by interval matrices, that is, $\Delta A_{\sigma(k)}^j(\Delta\xi) \in [\Delta A_{\sigma(k)}^j]$, $\Delta B_{\sigma(k)}^j(\Delta\xi) \in [\Delta B_{\sigma(k)}^j]$. Besides, it is assumed that the system states and input belong to the interval vectors $[X] = [\underline{x}, \bar{x}]$ and $[U] = [\underline{u}, \bar{u}]$, respectively, which can be represented by the following zonotopic sets:

$$\begin{aligned} x(k) \in \mathcal{X} &= \langle p_x, H_x \rangle, p_x = \text{mid}([X]), H_x = \text{rs}\left(\frac{\text{diam}([X])}{2}\right) \\ u(k) \in \mathcal{U} &= \langle p_u, H_u \rangle, p_u = \text{mid}([U]), H_u = \text{rs}\left(\frac{\text{diam}([U])}{2}\right) \end{aligned} \quad (9)$$

Thus, using Property 2, the uncertainty term can be described as follows:

$$\Delta A_{\sigma(k)}^j(\Delta\xi)x(k) + \Delta B_{\sigma(k)}^j(\Delta\xi)u(k) \in [\Delta A_{\sigma(k)}^j]\mathcal{X} \oplus [\Delta B_{\sigma(k)}^j]\mathcal{U} = \langle 0, E_{\theta,\sigma(k)}^j \rangle = \langle 0, [S_1 \ S_2 \ S_3 \ S_4] \rangle \quad (10)$$

where

$$S_1 = \text{seg}\left(\diamond([\Delta A_{\sigma(k)}^j]H_x)\right) = \text{rs}\left(\frac{\text{diam}([\Delta A_{\sigma(k)}^j])}{2}\right)|H_x| \quad (11a)$$

$$S_2 = \text{seg}\left(\diamond([\Delta B_{\sigma(k)}^j]H_u)\right) = \text{rs}\left(\frac{\text{diam}([\Delta B_{\sigma(k)}^j])}{2}\right)|H_u| \quad (11b)$$

$$S_3 = \frac{\text{diam}([\Delta A_{\sigma(k)}^j])}{2} p_x \quad (11c)$$

$$S_4 = \frac{\text{diam}([\Delta B_{\sigma(k)}^j])}{2} p_u \quad (11d)$$

Remark 1. It is worth noting that the intervals $[X]$ and $[U]$ may correspond to the theoretical maximum bounds or physical limits in the case of real applications.

4 | STATE ESTIMATION

In this section, we propose a set-membership state estimation approach for the SLPV system (1). This approach is based on parameterized intersection zonotope, which can be implemented by the following algorithm (Algorithm 1).

Algorithm 1. Set-membership state estimation algorithm

- 1. Prediction Step:** Given the SLPV system (5), compute the zonotopic uncertain state set $\bar{\mathcal{X}}_k = A_{\sigma(-)}(\rho(-))\hat{\mathcal{X}}_- \oplus B_{\sigma(-)}(\rho(-))u_- \oplus \sum_{j=1}^J h_{\sigma(-)}^j E_{\theta,\sigma(-)}(\rho(-)) \oplus E_w \mathcal{W}$, which bounds the set of predicted states.
 - 2. Measurement Step:** Compute the measurement state set \mathcal{X}_{y_k} by using the measurements y_k .
 - 3. Correction Step:** Compute the outer approximation $\hat{\mathcal{X}}_k$ of the intersection between $\bar{\mathcal{X}}_k$ and \mathcal{X}_{y_k} .
-

4.1 | Set-membership state estimation for SLPV system

The set-membership state estimation approach with zonotopes is now implemented by means of the following theorem.

Theorem 1. Given the switched discrete-time LPV system (5), let $\hat{\mathcal{X}}_k = \langle c_k, R_k \rangle \in \mathbb{R}^{n_x}$ be the zonotopic estimated state, where $c_k \in \mathbb{R}^{n_x}$ and $R_k \in \mathbb{R}^{n_x \times n_r}$ represent the center and generator matrix. Thus, $\downarrow_{q,W} R_k$ is the reduced generator matrix that is computed based on the Property 6. Assume that the initial state x_0 belongs to the set $\hat{\mathcal{X}}_0 = \langle c_0, R_0 \rangle$, the estimated state can be propagated as follows:

$$c_k = \bar{c}_k + \lambda_{\sigma(-)}(\rho(-))(y_k - C\bar{c}_k) \quad (12a)$$

$$R_k = \left[(I_{n_x} - \lambda_{\sigma(-)}(\rho(-))C)\bar{R}_k \quad \lambda_{\sigma(-)}(\rho(-))E_v \right] \quad (12b)$$

with

$$\bar{c}_k = A_{\sigma(-)}(\rho(-))c_- + B_{\sigma(-)}(\rho(-))u_- \quad (13a)$$

$$\bar{R}_k = \left[A_{\sigma(-)}(\rho(-)) \downarrow_{q,W} R_- \quad \sum_{j=1}^J h_{\sigma(-)}^j(\rho(-))E_{\theta,\sigma(-)}^j \quad E_w \right] \quad (13b)$$

where $\langle \bar{c}_k, \bar{R}_k \rangle$ represents the zonotopic set of predicted states.

Proof. Considering the SLPV system (5) with the inclusion $x_- \in \hat{\mathcal{X}}_- = \langle c_-, R_- \rangle$, the zonotopic predicted state set can be computed as:

$$\bar{\mathcal{X}}_k = \langle \bar{c}_k, \bar{R}_k \rangle = A_{\sigma(-)}(\rho(-)) \langle c_-, \downarrow_{q,W} R_- \rangle \oplus B_{\sigma(-)}(\rho(-)) \langle u(k), 0 \rangle \oplus \langle 0, E_{\theta,\sigma(-)}(\rho(-)) \rangle \oplus \langle 0, E_w \rangle \quad (14)$$

Then, consider the following polytopic form:

$$E_{\theta,\sigma(-)}(\rho(-)) = \sum_{j=1}^J h_{\sigma(-)}^j(\rho(-))E_{\theta,\sigma(-)}^j, \quad (15)$$

where \bar{c}_k and \bar{R}_k can be derived as in (13a,b).

In addition, the measurement state set \mathcal{X}_{y_k} is computed by considering current measurement y_k as

$$\mathcal{X}_{y_k} = \{x \in \mathbb{R}^{n_x} : |Cx - y_k| \leq E_v\} \quad (16)$$

Thus, the estimated state $\hat{\mathcal{X}}_k$ can be obtained through an outer approximation of the intersection between the zonotope (14) and the measurement state set (16). Based on the Property 5, the intersection zonotope is parameterized with a switched parameter-dependent correction matrix $\lambda_{\sigma(-)}(\rho(-)) \in \mathbb{R}^{n_x \times n_v}$, and given by:

$$\hat{\mathcal{X}}_k = \langle c_k, R_k \rangle = \langle \bar{c}_k + \lambda_{\sigma(-)}(\rho(-))(y_k - C\bar{c}_k), [(I_{n_x} - \lambda_{\sigma(-)}(\rho(-))C)\bar{R}_k \quad \lambda_{\sigma(-)}(\rho(-))E_v] \rangle \quad (17)$$

Therefore, the estimated state (12a,b) is derived. ■

4.2 | Optimal switched polytopic correction matrix design

As the correction matrix (also known as observer gain) directly affects the estimation performance, this section aims to find an optimal correction matrix $\lambda_i(\rho(-))$ such that minimizing the effects of uncertainties and restricting the size of the zonotopic state estimation set $\hat{\mathcal{X}}_k$ decreasing for all $i \in \mathcal{I}$ and all $k \geq 0$. According to Definition 3, the size of zonotopic state estimation set $\hat{\mathcal{X}}_k$ is measured by mode-dependent P_i -radius as follows:

$$l_{\sigma(-)}(k) = \max_{x_k \in \hat{\mathcal{X}}_k} \|x_k - c_k(\lambda_{\sigma(-)}(\rho(-)))\|_{P_{\sigma(-)}}^2 = \max_{z \in \mathbf{B}^{n_r}} \|R_k(\lambda_{\sigma(-)}(\rho(-)))z\|_{P_{\sigma(-)}}^2 \quad (18)$$

where $P_{\sigma(-)} = P_i \in \mathbb{R}^{n_x \times n_x} > 0, \forall i \in \mathcal{I}$ is the symmetric weighting matrix for the i^{th} subsystem.

As stated above, an optimal design of the correction matrix $\lambda_{\sigma(-)}(\rho(-))$ is required to minimize the effects of uncertainties and guarantee that the size of the zonotopic intersection is not increasing. In this context, the following conditions are proposed to limit the size of $\hat{\mathcal{X}}_k$ while considering the switching signal.

Lemma 2. *Given the switched system (5), if there exist scalars $\varepsilon_{\sigma(k)} \in (0, 1)$ and $\gamma_{\sigma(k)}$ associated with each subsystem $\sigma(k) = i$, constants $\alpha_2 > \alpha_1 > 0$ such that*

$$\forall \sigma(k) = i \in \mathcal{I}, \alpha_1 \Omega_i(+)) \leq l_i(+)) \leq \alpha_2 \Omega_i(+)), \quad (19)$$

$$l_i(+)) \leq \varepsilon_i l_i(k) + \gamma_i \delta_i \quad (20)$$

where $\alpha_1 = \min \text{eig}(P_i)$, $\alpha_2 = \max \text{eig}(P_i)$, $\Omega_i(k) = \max_{x_k \in \hat{\mathcal{X}}_k} \|x_k - c_k(\lambda_i(\rho(-)))\|$, δ_i is a positive switched constant that represents the maximum influence of process disturbance, parametric uncertainty and measurement noises as follows:

$$\delta_i = \max_{s_1 \in \mathbf{B}^{n_\theta}} \|E_{\theta,i}(\rho(-))s_1\|_2^2 + \max_{s_2 \in \mathbf{B}^{n_x}} \|E_{10}s_2\|_2^2 + \max_{s_3 \in \mathbf{B}^{n_y}} \|E_{11}s_3\|_2^2. \quad (21)$$

Then, the radius of the intersection zonotope $\hat{\mathcal{X}}_k$ is bounded and decreased for any switching signal with ADT

$$\tau_a > \tau_a^* = -\ln \mu / \ln(\varepsilon_i), \mu = \alpha_2 / \alpha_1. \quad (22)$$

Proof. Considering the inequality (20), we have

$$l_i(+)) \leq \varepsilon_i l_i(k) \leq \varepsilon_i l_i(k) + \gamma_i \delta_i \quad (23)$$

$\forall k-1 \in [k_l, k_{l+1})$, the i^{th} subsystem is active, for all $i, q \in \mathcal{I} \times \mathcal{I}, i \neq q$, leading to

$$l_i(-)) \leq \varepsilon_i^{k-k_l-1} l_i(k_l) \leq \varepsilon_i^{k-k_l-1} \frac{l_i(k_l)}{l_q(k_l)} l_q(k_l), \quad (24)$$

where

$$l_i(k_l) = \max_{x_{k_l} \in \hat{\mathcal{X}}_{k_l}} \|x_{k_l} - c_{k_l}(\lambda_i(\rho(k_l-1)))\|_{P_i}^2, \quad (25)$$

$$l_q(k_l) = \max_{x_{k_l} \in \hat{\mathcal{X}}_{k_l}} \|x_{k_l} - c_{k_l}(\lambda_q(\rho(k_l-1)))\|_{P_q}^2. \quad (26)$$

Since $\alpha_1 I_{n_x} \leq P_i \leq \alpha_2 I_{n_x}$, $\alpha_1 I_{n_x} \leq P_q \leq \alpha_2 I_{n_x}$, using condition (19), we have

$$\alpha_1 \Omega_i(k_l) \leq l_i(k_l) \leq \alpha_2 \Omega_i(k_l) \quad (27)$$

$$\alpha_1 \Omega_q(k_l) \leq l_q(k_l) \leq \alpha_2 \Omega_q(k_l) \quad (28)$$

with

$$\Omega_i(k_l) = \max_{x_{k_l} \in \hat{\mathcal{X}}_{k_l}} \|x_{k_l} - c_{k_l}(\lambda_i(\rho(k_l-1)))\|,$$

$$\Omega_q(k_l) = \max_{x_{k_l} \in \hat{\mathcal{X}}_{k_l}} \|x_{k_l} - c_{k_l}(\lambda_q(\rho(k_l-1)))\|,$$

where the zonotope $\hat{\mathcal{X}}_{k_l}$ and the centers $c_{k_l}(\lambda_i(\rho(k_l-1)))$ and $c_{k_l}(\lambda_q(\rho(k_l-1)))$ are shown schematically in Figure 2.

As $c_{k_l}(\lambda_i(\rho(k_l-1))) \neq c_{k_l}(\lambda_q(\rho(k_l-1)))$, it follows that

$$\Omega_i(k_l) < \Omega_q(k_l). \quad (29)$$

Thus, inequality (24) becomes

$$l_i(-)) \leq \varepsilon_i^{k-k_l-1} \frac{\alpha_2 \Omega_i(k_l)}{\alpha_1 \Omega_q(k_l)} l_q(k_l) \leq \varepsilon_i^{k-k_l-1} \frac{\alpha_2}{\alpha_1} l_q(k_l) \quad (30)$$

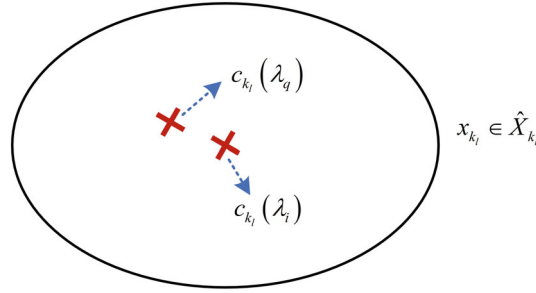


FIGURE 2 Centers at switching instant.

At the switching time instant $k - 1 = k_l$, it yields

$$l_i(k_l) \leq \mu l_q(k_l) \quad (31)$$

where $\mu = \frac{\alpha_2}{\alpha_1} > 1$. Therefore, the size of the intersection zonotope is decreasing for each subsystem, and bounded when the subsystem switches, which ends the proof. ■

If (20) holds, when $k \rightarrow \infty$, $l_\infty = \varepsilon_i l_\infty + \gamma_i \delta_i$, it follows that

$$l_\infty = \gamma_i \frac{\delta_i}{1 - \varepsilon_i}. \quad (32)$$

Equation (32) shows the equality of minimizing the P_i -radius (18), for given ε_i and δ_i , and minimizing the attenuation gain γ_i for all $i \in \mathcal{I}$. Then, the design of the parameter-dependent correction matrix $\lambda_i(\rho(k))$ associated with each subsystem involves solving a Multi-Objective Global Minimum Optimization problem with LMIs constraints according to the following theorem.

Theorem 2. Inequality (19) and (20) hold, if there exist a matrix $W_i^j \in \mathbb{R}^{n_x \times n_y}$, a positive definite matrix $P_i^j \in \mathbb{R}^{n_x \times n_x}$, scalars $\gamma > 0$, $\gamma_i^j > 0$ for given scalar $\varepsilon_i \in (0, 1)$ that are obtained by solving the following LMI optimization problem

$$\begin{aligned} & \min_{W_i^j, P_i^j, \gamma_i^j} \gamma \\ & \gamma_i^j \leq \gamma \end{aligned} \quad (33a)$$

$$\alpha_1 < P_i^j < \alpha_2 \quad (33b)$$

$$\begin{bmatrix} \varepsilon_i P_i^j & * & * & * & * \\ 0 & \gamma_i^j E_{\theta,i}^T E_{\theta,i} & * & * & * \\ 0 & 0 & \gamma_i^j E_w^T E_w & * & * \\ 0 & 0 & 0 & \gamma_i^j E_v^T E_v & * \\ (P_i^j - W_i^j C) A_i^j & (P_i^j - W_i^j C) E_{\theta,i}^j & (P_i^j - W_i^j C) E_w & W_i^j E_v & P_i^j \end{bmatrix} > 0 \quad (33c)$$

where $W_i^j = P_i^j \lambda_i^j$, $\lambda_i^j = P_i^{j-1} W_i^j$.

Then, the SMA estimator can estimate the zonotopic bound of the state for any switching signal with ADT satisfying (22). Besides, the estimation error is convergent and bounded by (32).

Proof. For all $\sigma(k) = i \in \mathcal{I}$, by denoting $\hat{z} = [z^T \quad s^T]^T$, $s = [s_1^T \quad s_2^T \quad s_3^T]^T$, where $z \in \mathbf{B}^{n_r}$, $s_1 \in \mathbf{B}^{n_\theta}$, $s_2 \in \mathbf{B}^{n_x}$, $s_3 \in \mathbf{B}^{n_y}$, (20) can be rewritten as

$$\max_{\hat{z} \in \mathbf{B}^{n_r + n_\theta + n_x + n_y}} \|R_+(\lambda_i(\rho(k)))\hat{z}\|_{P_i}^2 \leq \varepsilon_i \max_{z \in \mathbf{B}^{n_r}} \|R_k(\lambda_i(\rho(-)))z\|_{P_i}^2 + \gamma_i \left(\max_{s_1 \in \mathbf{B}^{n_\theta}} \|E_{\theta,i}(\rho(-))s_1\|_2^2 + \max_{s_2 \in \mathbf{B}^{n_x}} \|E_w s_2\|_2^2 + \max_{s_3 \in \mathbf{B}^{n_y}} \|E_v s_3\|_2^2 \right)$$

It follows that

$$\max_{\hat{z} \in \mathbf{B}^{n_r+n_\theta+n_x+n_y}} (\|R_+(\lambda_i(\rho(k)))\hat{z}\|_{P_i}^2 - \varepsilon_i \|R_k(\lambda_i(\rho(-)))\|_{P_i}^2 - \gamma_i (\|E_{\theta,i}(\rho(-))s_1\|_2^2 + \|E_w s_2\|_2^2 + \|E_v s_3\|_2^2)) \leq 0$$

which is equivalent to the following inequality:

$$\hat{z}^T R_+(\lambda_i(\rho(k)))^T P_i R_+(\lambda_i(\rho(k))) \hat{z} - \gamma_i s^T \Lambda_i s - \varepsilon_i z^T R_k(\lambda_i(\rho(-)))^T P_i R_k(\lambda_i(\rho(-))) z \leq 0 \quad (34)$$

where

$$\Lambda_i = \text{diag} \left(\begin{bmatrix} E_{\theta,i}(\rho(-))^T E_{\theta,i}(\rho(-)) & E_w^T E_w & E_v^T E_v \end{bmatrix} \right)$$

Recalling that

$$\begin{aligned} R_+(\lambda_i(\rho(k)))\hat{z} &= (I_{n_x} - \lambda_i(\rho(-))C)A_i(\rho(-))R_k(\lambda_i(\rho(-)))z \\ &\quad + [(I_{n_x} - \lambda_i(\rho(-))C)E_{\theta,i}(\rho(-))(I_{n_x} - \lambda_i(\rho(-))C)E_w \lambda_i(\rho(-))E_v]s, \end{aligned} \quad (35)$$

which allows to replace $R_+(\lambda_i(\rho(k)))\hat{z}$ in (34) with (35). Then, the following inequality (36) is derived,

$$\begin{bmatrix} R_k(\lambda_i(\rho(-)))z \\ s \end{bmatrix}^T \begin{bmatrix} A_i(\rho(-))^T (I_{n_x} - \lambda_i(\rho(-))C)^T P_i (I_{n_x} - \lambda_i(\rho(-))C) A_i(\rho(-)) - \varepsilon_i P_i & * \\ Z_i P_i (I_{n_x} - \lambda_i(\rho(-))C) A_i(\rho(-)) & Z_i P_i Z_i - \gamma_i \Lambda_i \end{bmatrix} \begin{bmatrix} R_k(\lambda_i(\rho(-)))z \\ s \end{bmatrix} \leq 0 \quad (36)$$

where

$$Z_i = \begin{bmatrix} (I_{n_x} - \lambda_i(\rho(-))C)E_{\theta,i} \\ (I_{n_x} - \lambda_i(\rho(-))C)E_w \\ \lambda_i(\rho(-))E_v \end{bmatrix}^T$$

Since inequality (36) holds, it is equivalent to that the following inequality (37) holds.

$$\begin{bmatrix} \varepsilon_i P_i & 0 \\ 0 & \gamma_i \Lambda_i \end{bmatrix} - \begin{bmatrix} ((I_{n_x} - \lambda_i(\rho(-))C)A_i(\rho(-)))^T P_i \\ Z_i P_i \end{bmatrix} P_i^{-1} \begin{bmatrix} ((I_{n_x} - \lambda_i(\rho(-))C)A_i(\rho(-)))^T P_i \\ Z_i P_i \end{bmatrix}^T > 0 \quad (37)$$

With the application of Schur complement, (37) can be rewritten as (38).

$$\begin{bmatrix} \varepsilon_i P_i & * & * & * & * \\ 0 & \gamma_i E_{\theta,i}(\rho(-))^T E_{\theta,i}(\rho(k)) & * & * & * \\ 0 & 0 & \gamma_i E_w^T E_w & * & * \\ 0 & 0 & 0 & \gamma_i E_v^T E_v & * \\ P_i((I_{n_x} - \lambda_i(\rho(-))C)A_i(\rho(-))) & P_i((I_{n_x} - \lambda_i(\rho(-))C)E_{\theta,i}(\rho(-))) & P_i((I_{n_x} - \lambda_i(\rho(-))C)E_w) & P_i(\lambda_i(\rho(-))E_v) & P_i \end{bmatrix} > 0 \quad (38)$$

Since $A_i(\rho(-))$, $B_i(\rho(-))$, $\lambda_i(\rho(-))$ and $E_{\theta,i}(\rho(-))$ are parameter-dependent, considering the following polytopic form,

$$\begin{aligned} A_i(\rho(-)) &= \sum_{j=1}^J h_i^j(\rho(-)) A_i^j, \\ B_i(\rho(-)) &= \sum_{j=1}^J h_i^j(\rho(-)) B_i^j, \\ E_{\theta,i}(\rho(-)) &= \sum_{j=1}^J h_i^j(\rho(-)) E_{\theta,i}^j, \\ \lambda_i(\rho(-)) &= \sum_{j=1}^J h_i^j(\rho(-)) \lambda_i^j, \end{aligned} \quad (39)$$

the following inequality holds for all vertices $\forall j \in J$:

$$\begin{bmatrix} \varepsilon_i P_i^j & * & * & * & * \\ 0 & \gamma_i^j E_{\theta,i}^j T E_{\theta,i}^j & * & * & * \\ 0 & 0 & \gamma_i^j E^T E & * & * \\ 0 & 0 & 0 & \gamma_i^j F^T F & * \\ P_i^j \left((I_{n_x} - \lambda_i^j) C \right) A_i^j & P_i^j \left((I_{n_x} - \lambda_i^j) C \right) E_{\theta,i}^j & P_i^j \left((I_{n_x} - \lambda_i^j) C \right) E & P_i^j \left(\lambda_i^j \right) F & P_i^j \end{bmatrix} \succ 0 \quad (40)$$

It is worth noting that the parameters P_i^j and γ_i^j are used in (40) to introduce more degrees of freedom and consequently reduce the conservatism. Then, (33c) can be derived by applying $W_i^j = P_i^j \lambda_i^j$, $\lambda_i^j = P_i^{j-1} W_i^j$. Therefore, by minimizing the gain γ_i , $\forall i \in \mathcal{I}$, the intersection zonotope $\hat{\mathcal{X}}_k$ can be made as tight as possible. In order to solve this multi-objective optimization problem, one objective scalar γ is minimized while the others are transformed into constraints $\gamma_i \leq \gamma$. Hence, this complete the proof. ■

5 | EXTENSION TO FAULT/DISTURBANCE ESTIMATION

In this section, we extend the proposed set-membership state estimation to fault/disturbance estimation for the SLPV system (5), in case of input disturbance, actuator fault or sensor fault, described as follows:

$$\begin{cases} x(k+1) = A_{\sigma(k)}(\rho(k))x(k) + B_{\sigma(k)}(\rho(k))u(k) + E_{\theta,\sigma(k)}(\rho(k))\theta(k) + F_a f_a(k)(\rho(k)) + E_w w(k) \\ y(k) = Cx(k) + F_s f_s(k) + E_v v(k) \end{cases}, \quad (41)$$

where $f_a \in \mathbb{R}^{n_{f_a}}$ and $f_s \in \mathbb{R}^{n_{f_s}}$ denote respectively the actuator fault/input disturbance and the sensor fault signal, $F_a \in \mathbb{R}^{n_x \times n_{f_a}}$ and $F_s \in \mathbb{R}^{n_y \times n_{f_s}}$ are corresponding matrices.

By means of a state augmentation technique, the system (41) is rewritten and the fault/disturbance vector is regarded as an extra state. Therefore, the proposed set-membership state estimation can be applied to estimate the corresponding fault/disturbance. In order to achieve fault/disturbance estimation, the following assumption is considered in this paper.

Assumption 1. The considered fault $f(k)$, generally referring to fault/disturbance signal, is piecewise constant or slow varying. Therefore, it is assumed that

$$f(k+1) = f(k) + \delta, \quad (42)$$

with known scalar δ .

Remark 2. As the actuator fault and input disturbance behave similarly and are mathematically represented the same, the following implementation method for actuator fault estimation or input disturbance estimation is the same. Consequently, in order to avoid complexity and reduce the content space, we combine the two scenarios together, denoting the actuator fault or the input disturbance by one variable f_a . Besides, n_f is employed to generally represent the dimension of the fault/disturbance vector, where $n_f \in \{n_{f_a}, n_{f_s}\}$. In the case of actuator fault estimation, $n_f = n_{f_a}$.

5.1 | Augmented descriptor SLPV system generation

In order to estimate the fault/disturbance vector $f_a(k)$ or $f_s(k)$, it is considered as an auxiliary state with the aid of an augmentation technique. Take the actuator fault $f_a(k)$ for example, the auxiliary state is represented as:

$$\bar{x}(k) = \begin{bmatrix} x(k) \\ f_a(k) \end{bmatrix} \in \mathbb{R}^{n_{\bar{x}}}, \quad n_{\bar{x}} = n_x + n_f.$$

Then, the system (41) is formulated as an augmented descriptor SLPV system constructed as follows:

$$\begin{cases} E\bar{x}(k+1) = \bar{A}_{\sigma(k)}(\rho(k))\bar{x}(k) + \bar{B}_{\sigma(k)}(\rho(k))u(k) + \bar{E}_{\theta,\sigma(k)}(\rho(k))\theta(k) + \bar{E}_w w(k) \\ y(k) = \bar{C}\bar{x}(k) + E_v v(k) \end{cases} \quad (43)$$

where

$$\begin{aligned} E &= \begin{bmatrix} I_{n_x} & -F_a \\ 0 & I_{n_f} \end{bmatrix}, & \bar{A}_{\sigma(k)}(\rho(k)) &= \begin{bmatrix} A_{\sigma(k)}(\rho(k)) & 0 \\ 0 & I_{n_f} \end{bmatrix}, & \bar{B}_{\sigma(k)}(\rho(k)) &= \begin{bmatrix} B_{\sigma(k)}(\rho(k)) \\ 0 \end{bmatrix}, \\ \bar{E}_{\theta,\sigma(k)}(\rho(k)) &= \begin{bmatrix} E_{\theta,\sigma(k)}(\rho(k)) \\ 0 \end{bmatrix}, & \bar{E}_w &= \begin{bmatrix} E_w \\ \delta \end{bmatrix}, & \bar{C} &= \begin{bmatrix} C & 0 \end{bmatrix} \end{aligned} \quad (44)$$

Remark 3. It is worth noting that when it comes to estimate the sensor fault $f_s(k)$, the corresponding auxiliary state and system matrices are defined as:

$$\bar{x}(k) = \begin{bmatrix} x(k) \\ f_s(k) \end{bmatrix}, \quad \bar{A}_{\sigma(k)}(\rho(k)) = \begin{bmatrix} A_{\sigma(k)}(\rho(k)) & 0 \\ 0 & I_{n_f} \end{bmatrix}, \quad \bar{C} = \begin{bmatrix} C & F_s \end{bmatrix}, \quad E = \begin{bmatrix} I_{n_x} & 0 \\ 0 & I_{n_f} \end{bmatrix} \quad (45)$$

Lemma 3 (Observability⁴⁶). *The descriptor SLPV system (43) is C-observable if and only if rank $\begin{bmatrix} zE - \bar{A}_{\sigma(k)}(\rho(k)) \\ \bar{C} \end{bmatrix} = n_{\bar{x}}, \forall z \in \mathbb{C}, z \text{ finite and rank } \begin{bmatrix} E \\ \bar{C} \end{bmatrix} = n_{\bar{x}}$.*

Remark 4. With observability premised, there is no theoretical issue of estimating multiple faults simultaneously with the proposed method. In case of estimating actuator and sensor faults simultaneously, we consider the augmented states as $\bar{x}(k) = [x^T(k) \ f_a^T(k) \ f_s^T(k)]^T$. However, the estimation performance would decrease as auxiliary states increase. The ideal situation is to employ the proposed method for single-fault estimation.

Therefore, the state estimation method proposed in the previous section is directly applicable as long as the augmented system (43) is observable. For the newly generated augmented descriptor system (43), the problem of fault/disturbance estimation is readily transformed into state estimation. Consequently, the proposed set-membership state estimation in Section 4 for SLPV systems is extended to the descriptor SLPV systems.

5.2 | Set-membership state estimation for augmented descriptor SLPV system

In what follows, the set-membership state estimation approach for the augmented descriptor SLPV system (43) is presented. The implementation is based on computing the outer approximation $\hat{\mathcal{X}}_k$ of the intersection between the predicted state set $\bar{\mathcal{X}}_k$ and the measurement state set \mathcal{X}_{y_k} , which is given below.

Theorem 3. *Given augmented switched discrete-time LPV system (43), let $\hat{\mathcal{X}}_k = \langle c_k, R_k \rangle \in \mathbb{R}^{n_x}$ be the zonotopic estimated state, where $c_k \in \mathbb{R}^{n_x}$ and $R_k \in \mathbb{R}^{n_x \times n_{R_k}}$ represent the center and shape matrix. Assume that the initial state \bar{x}_0 belongs to the set $\hat{\mathcal{X}}_0 = \langle c_0, R_0 \rangle$, the estimated state can be propagated as follows:*

$$c_k = \bar{c}_k + \lambda_{\sigma(-)}(\rho(-)) \left(y(k) - \bar{C}\bar{c}_k \right) \quad (46a)$$

$$R_k = \left[\left(I_{n_{\bar{x}}} - \lambda_{\sigma(-)}(\rho(-))\bar{C} \right) \bar{R}_k \quad \lambda_{\sigma(-)}(\rho(-))E_v \right] \quad (46b)$$

with

$$\bar{c}_k = T\bar{A}_{\sigma(-)}(\rho(-))c_- + T\bar{B}_{\sigma(-)}(\rho(-))u(-) + Ny(k) \quad (47a)$$

$$\bar{R}_k = \left[T\bar{A}_{\sigma(-)}(\rho(-)) \downarrow_{q,W} R_- \quad \sum_{j=1}^J h_{\sigma(-)}^j(\rho(-))T\bar{E}_{\theta,\sigma(-)}^j \quad T\bar{E}_w \quad NE_v \right] \quad (47b)$$

where $\langle \bar{c}_k, \bar{R}_k \rangle = \bar{\mathcal{X}}_k$ represents the zonotopic set of predicted states, $\lambda_{\sigma}(\rho(k))$ is the correction matrix, $T \in \mathbb{R}^{n_{\bar{x}} \times n_{\bar{x}}}$ and $N \in \mathbb{R}^{n_{\bar{x}} \times n_y}$ are constant matrices designed to satisfy

$$TE + N\bar{C} = I_{n_{\bar{x}}} \quad (48)$$

According to Lemma 1, the general solution of (48) is given by:

$$\begin{aligned} T &= \Psi^\dagger a_1 + S(I_{n_x} - \Psi\Psi^\dagger) a_1, \\ N &= \Psi^\dagger a_2 + S(I_{n_x} - \Psi\Psi^\dagger) a_2, \end{aligned} \quad (49)$$

$$\text{with } \Psi = \begin{bmatrix} E \\ C \end{bmatrix}, a_1 = \begin{bmatrix} I_{n_x} \\ 0 \end{bmatrix} \text{ and } a_2 = \begin{bmatrix} 0 \\ I_{n_f} \end{bmatrix}.$$

Proof. Given a pair of matrices T and N satisfying (48), for system (43), we have

$$\begin{aligned} \bar{x}(k) &= (TE + N\bar{C})\bar{x}(k) = T\bar{A}_{\sigma(-)}(\rho(-))\bar{x}(-) + T\bar{B}_{\sigma(-)}(\rho(-))u(-) + T\bar{E}_{\theta,\sigma(-)}(\rho(-))\theta(-) + Ny(k) \\ &\quad + T\bar{E}_w w(-) - NE_v v(k) \end{aligned} \quad (50)$$

By considering the inclusion $\bar{x}(-) \in \hat{\mathcal{X}}_- = \langle c_-, R_- \rangle \subseteq \langle c_-, \downarrow_{q,w} R_- \rangle$, and the polytopic form (15), the zonotopic predicted states set can be computed as:

$$\bar{\mathcal{X}}_k = T\bar{A}_{\sigma(-)}(\rho(-))\langle c_-, R_- \rangle \oplus \langle T\bar{B}_{\sigma(-)}(\rho(-))u(-), 0 \rangle \oplus \langle Ny(k), 0 \rangle \oplus \left\langle 0, \sum_{j=1}^J h_{\sigma(-)}^j(\rho(-))T\bar{E}_{\theta,\sigma(-)}^j \right\rangle \oplus \langle 0, T\bar{E}_w \rangle \oplus \langle 0, NE_v \rangle, \quad (51)$$

which can be represented as (47a,b).

Then, similar to the proof of Theorem 1, the estimated state $\hat{\mathcal{X}}_k$ can be obtained through an outer approximation of the intersection between the zonotope (51) and the measurement state set \mathcal{X}_{y_k} , denoted by $\mathcal{X}_{y_k} = \left\{ x \in \mathbb{R}^{n_x} : \left| \bar{C}\bar{x}(k) - y(k) \right| \leq E_v \right\}$. Based on the Property 5, (46a,b) is obtained and the proof is complete. ■

5.3 | Optimal switched polytopic correction matrix design

Following the same methodology as in the previous section, the optimal design for $\lambda_{\sigma(-)}(\rho(-))$ aims to measure the size of zonotopic state estimation set $\hat{\mathcal{X}}_k$, which is measured by mode-dependent P_i -radius as follows:

$$l_{\sigma(-)}(k) = \max_{x_k \in \hat{\mathcal{X}}_k} \|x_k - c_k(\lambda_{\sigma(-)}(\rho(-)))\|_{P_{\sigma(-)}}^2 = \max_{z \in \mathbf{B}^{n_r}} \|R_k(\lambda_{\sigma(-)}(\rho(-)))z\|_{P_{\sigma(-)}}^2 \quad (52)$$

where $P_{\sigma(-)} = P_i, \forall i \in \mathcal{I}$ is the weighting matrix for the i^{th} subsystem. If there exist scalars $\varepsilon_{\sigma(k)} \in (0, 1)$ and $\gamma_{\sigma(k)}$ associated with each subsystem $\sigma(k) = i$, constants $\alpha_2 > \alpha_1 > 0$ such that

$$\forall \sigma(k) = i \in \mathcal{I}, \alpha_1 \Omega_i(+) \leq l_i(+) \leq \alpha_2 \Omega_i(+), \quad (53)$$

$$l_i(k+1) \leq \varepsilon_i l_i(k) + \gamma_i \delta_i \quad (54)$$

where $\alpha_1 = \min \text{eig}(P_i)$, $\alpha_2 = \max \text{eig}(P_i)$, $\Omega_i(k) = \max_{x_k \in \hat{\mathcal{X}}_k} \|x_k - c_k(\lambda_i(\rho(-)))\|$, δ_i is a positive switched constant that represents the maximum influence of process disturbance, parametric uncertainty and measurement noises as follows:

$$\delta_i = \max_{s_1 \in \mathbf{B}^{n_\theta}} \|\bar{E}_{\theta,i}(\rho(-))s_1\|_2^2 + \max_{s_2 \in \mathbf{B}^{n_w}} \|\bar{E}_w s_2\|_2^2 + \max_{s_3 \in \mathbf{B}^{n_y}} \|E_v s_3\|_2^2. \quad (55)$$

Then, the radius of the intersection zonotope $\hat{\mathcal{X}}_k$ is convergent and stable for any switching signal with ADT

$$\tau_a > \tau_a^* = -\ln \mu / \ln(\varepsilon_i), \mu = \alpha_2 / \alpha_1. \quad (56)$$

Therefore, when $k \rightarrow \infty$, $l_\infty = \varepsilon_i l_\infty + \gamma_i \delta_i$, it follows that $l_\infty = \gamma_i \frac{\delta_i}{1 - \varepsilon_i}$, which reveals that $\forall i \in \mathcal{I}$, a smaller gain γ_i provides a tighter information in terms of the effect of ε_i . This leads to solve the following optimization problem:

Theorem 4. Inequality (53) and (54) hold, if there exist a matrix $W_i^j \in \mathbb{R}^{n_x \times n_y}$, a positive definite matrix $P_i^j \in \mathbb{R}^{n_x \times n_x}$, scalars $\gamma > 0, \gamma_i^j > 0$ for given scalars $\varepsilon_i \in (0, 1)$ such that the following LMI optimization problem holds

$$\begin{aligned} & \min_{W_i^j, \gamma_i^j, \gamma_i} \gamma \\ & \gamma_i^j \leq \gamma \end{aligned} \quad (57a)$$

$$\alpha_1 < P_i^j < \alpha_2 \quad (57b)$$

$$\begin{bmatrix} \varepsilon_i P_i^j & * & * & * & * & * \\ 0 & \gamma_i^j \bar{E}_{\theta,i}^T \bar{E}_{\theta,i}^j & * & * & * & * \\ 0 & 0 & \gamma_i^j \bar{E}_w^T \bar{E}_w & * & * & * \\ 0 & 0 & 0 & \gamma_i^j E_v^T E_v & * & * \\ 0 & 0 & 0 & 0 & 0 & * \\ (P_i^j - W_i^j \bar{C}_i) T \bar{A}_i^j & (P_i^j - W_i^j \bar{C}_i) T \bar{E}_{\theta,i}^j & (P_i^j - W_i^j \bar{C}_i) T \bar{E}_w & W_i^j E_v & (P_i^j - W_i^j \bar{C}_i) N E_v & P_i^j \end{bmatrix} > 0 \quad (57c)$$

where $W_i^j = P_i^j \lambda_i^j$, $\lambda_i^j = P_i^{j-1} W_i^j$.

Proof. Let $\hat{z} = [z^T \quad s^T]^T$, $s = [s_1^T \quad s_2^T \quad s_3^T \quad s_4^T]^T$, where $z \in \mathbf{B}^{n_r}$, $s_1 \in \mathbf{B}^{n_\theta}$, $s_2 \in \mathbf{B}^{n_x}$, $s_3 \in \mathbf{B}^{n_y}$, $s_4 \in \mathbf{B}^{n_y}$, $\forall \sigma(k) = i \in \mathcal{I}$, using (54) we have

$$\max_{\hat{z} \in \mathbf{B}^{n_r+n_\theta+n_x+2n_y}} \|R_+(\lambda_i(\rho(k)))\hat{z}\|_{P_i}^2 \leq \varepsilon_i \max_{z \in \mathbf{B}^{n_r}} \|R_-(\lambda_i(\rho(k)))z\|_{P_i}^2 + \gamma_i (\max_{s_1 \in \mathbf{B}^{n_\theta}} \|\bar{E}_{\theta,i}(\rho(-))s_1\|_2^2 + \max_{s_2 \in \mathbf{B}^{n_x}} \|\bar{E}_w s_2\|_2^2 + \max_{s_3 \in \mathbf{B}^{n_y}} \|E_v s_3\|_2^2).$$

It is equivalent to the following inequality:

$$\max_{\hat{z}} (\hat{z}^T R_+(\lambda_i(\rho(k)))^T P_i R_+(\lambda_i(\rho(k))) - \begin{bmatrix} \varepsilon_i R_k(\lambda_i(\rho(-)))^T P_i R_k(\lambda_i(\rho(-))) & 0 & 0 & 0 & 0 \\ 0 & \gamma_i \bar{E}_{\theta,i}(\rho(-))^T \bar{E}_{\theta,i}(\rho(-)) & 0 & 0 & 0 \\ 0 & 0 & \gamma_i \bar{E}_w^T \bar{E}_w & 0 & 0 \\ 0 & 0 & 0 & \gamma_i E_v^T E_v & 0 \\ 0 & 0 & 0 & 0 & 0 \end{bmatrix} \hat{z}) < 0 \quad (58)$$

Replacing $R_+(\lambda_i(\rho(k)))\hat{z}$ in (58) by recalling $R_+(\lambda_i(\rho(k)))\hat{z} = Z_i \hat{z}$, where

$$Z_i = \begin{bmatrix} (I_{n_x} - \lambda_i(\rho(-))\bar{C}) T \bar{A}_i(\rho(-)) & (I_{n_x} - \lambda_i(\rho(-))\bar{C}) T \bar{E}_{\theta,i}(\rho(-)) & (I_{n_x} - \lambda_i(\rho(-))\bar{C}) T \bar{E}_w & (I_{n_x} - \lambda_i(\rho(-))\bar{C}) N E_v & \lambda_i(\rho(-)) E_v \end{bmatrix},$$

it leads to:

$$\begin{bmatrix} R_k(\lambda_i(\rho(-)))z \\ s \end{bmatrix}^T \left(Z_i^T P_i Z_i - \begin{bmatrix} \varepsilon_i P_i & 0 & 0 & 0 & 0 \\ 0 & \gamma_i \bar{E}_{\theta,i}(\rho(-))^T \bar{E}_{\theta,i}(\rho(-)) & 0 & 0 & 0 \\ 0 & 0 & \gamma_i \bar{E}_w^T \bar{E}_w & 0 & 0 \\ 0 & 0 & 0 & \gamma_i E_v^T E_v & 0 \\ 0 & 0 & 0 & 0 & 0 \end{bmatrix} \right) \begin{bmatrix} R_k(\lambda_i(\rho(-)))z \\ s \end{bmatrix} < 0 \quad (59)$$

Since inequality (59) holds, it is equivalent to that the following inequality (60) holds.

$$\begin{bmatrix} \varepsilon_i P_i & 0 & 0 & 0 & 0 \\ 0 & \gamma_i \bar{E}_{\theta,i}(\rho(-))^T \bar{E}_{\theta,i}(\rho(-)) & 0 & 0 & 0 \\ 0 & 0 & \gamma_i \bar{E}_w^T \bar{E}_w & 0 & 0 \\ 0 & 0 & 0 & \gamma_i E_v^T E_v & 0 \\ 0 & 0 & 0 & 0 & 0 \end{bmatrix} - Z_i^T P_i Z_i > 0 \quad (60)$$

With the application of Schur complement for (60), and considering polytopic form, the following inequality holds for all vertices $\forall j \in J$:

$$\begin{bmatrix} \varepsilon_i P_i^j & * & * & * & * & * \\ 0 & \gamma_i \bar{E}_{\theta,i}^{jT} \bar{E}_{\theta,i}^j & * & * & * & * \\ 0 & 0 & \gamma_i \bar{E}_w^T \bar{E}_w & * & * & * \\ 0 & 0 & 0 & \gamma_i E_v^T E_v & * & * \\ 0 & 0 & 0 & 0 & 0 & * \\ P_i^j \left((I_{n_x} - \lambda_i^j \bar{C}) T \bar{A}_i \right) & P_i^j \left((I_{n_x} - \lambda_i^j \bar{C}) T \bar{E}_{\theta,i}^j \right) & P_i^j \left((I_{n_x} - \lambda_i^j \bar{C}) N E_v \right) & P_i^j \left((I_{n_x} - \lambda_i^j \bar{C}) \bar{E}_w \right) & P_i^j \left(\lambda_i^j E_v \right) & P_i^j \end{bmatrix} > 0 \quad (61)$$

Here, we also employ the vertices P_i^j and γ_i^j for more degrees of freedom. Then, (57c) can be derived by applying $W_i^j = P_i^j \lambda_i^j$, $\lambda_i^j = P_i^{j-1} W_i^j$. Therefore, by introducing (57a), the size of the intersection zonotope $\hat{\lambda}_k$ can be sought as tight as possible. Hence, the proof is completed. ■

With the set-membership state estimator for fault/disturbance estimation designed in Theorem 3 and the optimal correction matrix in Theorem 4, we summarize the fault/disturbance estimation algorithm in Algorithm 2.

Algorithm 2. Fault/disturbance estimation algorithm for augmented SLPV system

Given the system matrices, S , ε_i , the system input, states and the initial state bounded in $x(t) \in [\underline{x}, \bar{x}]$, $u(t) \in [\underline{u}, \bar{u}]$, $x_0 \in \langle c_0, R_0 \rangle$;

Compute parameter uncertainty using (10);

Generate the augmented SLPV system (43);

Solve Equation~(48) to obtain T and N ;

Solve the optimization problem (57c) to obtain the optimal correction matrix λ_i^j ;

for $1 < k < K$ **do**

 Compute the predicted states zonotope $\langle \bar{c}_k, \bar{R}_k \rangle$ by using (47);

 Compute the state estimation zonotope $\langle c_k, R_k \rangle$ by using (46);

 Obtain the fault estimation zonotope $\langle c_k^f, R_k^f \rangle = [0 \quad I_{n_f}] \langle c_k, R_k \rangle$ with its bounds $\hat{f}_i(k) \in [f_{-i}^f(k), \bar{f}_i^f(k)]$, $i = 1, \dots, n_f$

with

$$\hat{f}(k) = c_k^f,$$

$$\hat{f}_i(k) = c_k^f(i),$$

$$\bar{f}_i(k) = \hat{f}_i(k) + \text{rs} \left(R_k^f \right)_{i,i},$$

$$f_{-i}^f(k) = \hat{f}_i(k) - \text{rs} \left(R_k^f \right)_{i,i},$$

$$e_f(k) = f(k) - \hat{f}(k),$$

 where $e_f(k)$ is the fault estimation error vector.

end for

6 | CASE STUDY

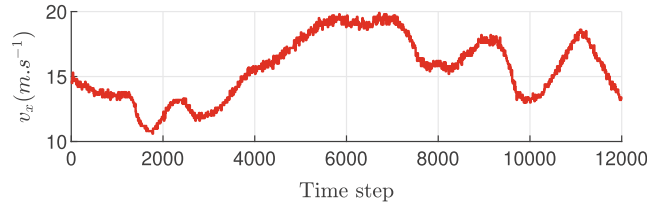
In this section, the following vehicle lateral dynamic model is employed to demonstrate the effectiveness of the proposed estimation approach

$$\begin{bmatrix} \dot{\beta} \\ \dot{\psi} \end{bmatrix} = \begin{bmatrix} -\frac{c_f + c_r}{m v_x} & \frac{c_r l_r - c_f l_f}{m v_x^2} - 1 \\ \frac{c_r l_r - c_f l_f}{I_z} & -\frac{c_r l_r^2 + c_f l_f^2}{I_z v_x} \end{bmatrix} \begin{bmatrix} \beta \\ \psi \end{bmatrix} + \begin{bmatrix} c_f \\ \frac{m v_x}{I_z} \\ \frac{c_r l_f}{I_z} \end{bmatrix} \delta_f \quad (62)$$

where the system states β and ψ denote the sideslip angle and yaw rate; input δ_f denotes the steering angle; the longitudinal velocity v_x and the cornering stiffness c_f , c_r are selected as the measurable and unmeasurable but bounded scheduling variables respectively. It is worth noting that the cornering stiffness parameters c_f and c_r are not measurable and vary with the surface friction. For a more precise model, readjustment variables Δc_r and Δc_f are taken into account to correct the

TABLE 1 System parameter.

Parameter	Description	Value	Unit
m	Mass	1600	kg
I_z	Yaw moment	2454	kg · m ²
l_f	Distance from front axle to the center of gravity.	1	m
l_r	Distance from rear axle to the center of gravity.	1.44	m
c_f	Cornering stiffness of front tires	35,468	N/rad
c_r	Cornering stiffness of rear tires	40,057	N/rad

FIGURE 3 Longitudinal velocity v_x .

wheel cornering stiffness errors as: $c_f = c_{f0} + \Delta c_f$ and $c_r = c_{r0} + \Delta c_r$, where c_{f0} and c_{r0} represent known nominal values, and Δc_r and Δc_f are assumed to be unknown but bounded, satisfying $|\Delta c_r| \leq 0.1c_{r0}$, $|\Delta c_f| \leq 0.1c_{f0}$. System parameters and nominal values are described in Table 1. Given a sampling time $T = 0.01s$, a discrete-time LPV model of the system (62), subject to parameter uncertainties and noises, can be obtained by Euler's discretization method as follows:

$$\begin{cases} x(+) = A(\rho(k), \xi(k))x(k) + B(\rho(k), \xi(k))u(k) + E_w w(k) \\ y(k) = Cx(k) + E_v v(k) \end{cases} \quad (63)$$

where

$$A(\rho(k), \xi(k)) = I_{n_x} + T \begin{bmatrix} -\frac{c_f + c_r}{mv_x} & \frac{c_r l_r - c_f l_f}{mv_x^2} - 1 \\ \frac{c_r l_r - c_f l_f}{I_z} & -\frac{c_r l_r^2 + c_f l_f^2}{I_z v_x} \end{bmatrix}, \quad B(\rho(k), \xi(k)) = T \begin{bmatrix} \frac{c_f}{mv_x} \\ \frac{c_f l_f}{I_z} \end{bmatrix}.$$

In the present study, the following simulation data are used: the measurable scheduling variable $\rho(k) = v_x$ depicted in Figure 3, the unmeasurable scheduling variable $\xi(k) = [c_r \quad c_f]^T$, $C = [0 \quad 1]$, $E_w = \begin{bmatrix} 0.001 & 0 \\ 0 & 0.02 \end{bmatrix}$, $E_v = 0.03$, and the system disturbances w and measurement noise v are random white noise bounded in zonotopes: $w \in \mathcal{W} = \langle 0, I_2 \rangle$, $v \in \mathcal{V} = \langle 0, I_1 \rangle$.

Considering the characteristic of the measured longitudinal velocity v_x in Figure 3, the whole parameter space can be divided into three sub-regions according to the following switching rule:

$$\sigma(k) = \begin{cases} 1 & \text{if } 9m \cdot s^{-1} < v_x \leq 13.4m \cdot s^{-1} \\ 2 & \text{if } 13.4m \cdot s^{-1} < v_x \leq 16.5m \cdot s^{-1} \\ 3 & \text{if } 16.5m \cdot s^{-1} < v_x \leq 20m \cdot s^{-1} \end{cases} \quad (64)$$

and three local models are obtained with the considered switching law as shown in Figure 4. Furthermore, to decouple the uncertainties on the parameter $\xi(k)$, the system matrices can be represented as (3). Approximating the uncertainties on system matrices by an uncertain term $E_{\theta, \sigma(k)}(\rho(k))\theta(k)$ and using the sector nonlinearity approach, a switched polytopic LPV system with three subsystems and two submodels for each subsystem is derived and given as follows:

$$\begin{cases} x(+) = \sum_{j=1}^2 h_{\sigma(k)}^j(\rho(k))(A_{\sigma(k)}^j x(k) + B_{\sigma(k)}^j u(k) + E_{\theta, \sigma(k)}^j \theta(k)) + E_w w(k) \\ y(k) = Cx(k) + E_v v(k) \end{cases} \quad (65)$$

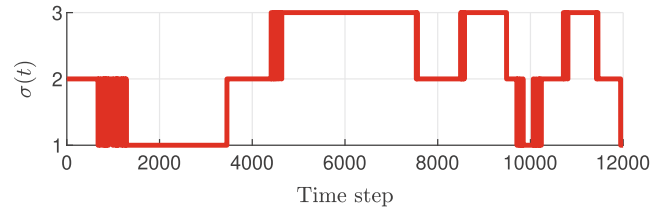


FIGURE 4 Switching signal $\sigma(k)$.

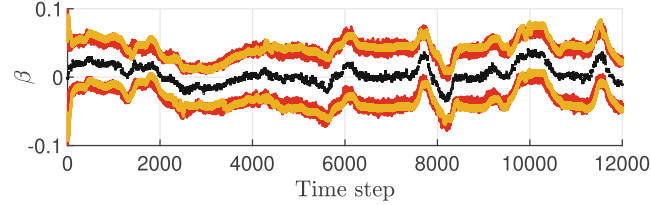


FIGURE 5 Set-membership estimation of side slip angle using proposed approach (red) and reference approach (orange).

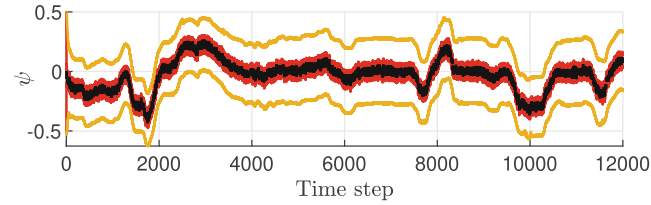


FIGURE 6 Set-membership estimation of yaw rate using proposed approach (red) and reference approach (orange).

where

$$\begin{aligned}
 A_1^1 &= \begin{bmatrix} 0.9648 & -0.0092 \\ 0.0905 & 0.9640 \end{bmatrix}, & A_1^2 &= \begin{bmatrix} 0.9555 & -0.0088 \\ 0.0905 & 0.9544 \end{bmatrix}, & B_1^1 &= \begin{bmatrix} 0.0165 \\ 0.1445 \end{bmatrix}, & B_1^2 &= \begin{bmatrix} 0.0209 \\ 0.1445 \end{bmatrix}, \\
 A_2^1 &= \begin{bmatrix} 0.9714 & -0.0095 \\ 0.0905 & 0.9707 \end{bmatrix}, & A_2^2 &= \begin{bmatrix} 0.9648 & -0.0092 \\ 0.0905 & 0.9640 \end{bmatrix}, & B_2^1 &= \begin{bmatrix} 0.0134 \\ 0.1445 \end{bmatrix}, & B_2^2 &= \begin{bmatrix} 0.0165 \\ 0.1445 \end{bmatrix}, \\
 A_3^1 &= \begin{bmatrix} 0.9763 & -0.0096 \\ 0.0905 & 0.9757 \end{bmatrix}, & A_3^2 &= \begin{bmatrix} 0.9714 & -0.0095 \\ 0.0905 & 0.9707 \end{bmatrix}, & B_3^1 &= \begin{bmatrix} 0.0111 \\ 0.1445 \end{bmatrix}, & B_3^2 &= \begin{bmatrix} 0.0134 \\ 0.1445 \end{bmatrix},
 \end{aligned}$$

In this paper, the system states and input belong to the interval vectors $[X(1)] = [-0.06, 0.06]$, $[X(2)] = [-0.5, 0.4]$ and $[U] = [-0.14, 0.08]$. Therefore, $E_{\theta, \sigma(k)}^j$ can be computed based on (10). Due to the space limitation, the details of matrix $E_{\theta, \sigma(k)}^j$ are omitted.

6.1 | Simulation 1: State estimation

By solving the LMI optimization problem (33) and selecting the scalar $\varepsilon_i = 0.78$, we can obtain the switched polytopic correction matrices $\lambda_{\sigma(k)}^j$ and the corresponding minimum ADT $\tau_a^* = 8.7985$ through (22). Then, the actual trajectories of the system states (black line) and the state-bounding intervals (red line) are depicted in Figures 5 and 6. Furthermore, with the same parameter settings, a comparison is conducted using the SMA-based switched state estimator proposed in Reference 28 for the system (5). As seen from the compared estimation results shown in Figures 5 and 6, the proposed method allows to provide a more accurate bounded estimation of the vehicle state variables, thus less conservative.

6.2 | Simulation 2: Actuator fault estimation

In case of an actuator fault occurrence, a faulty switched polytopic LPV model, following (65), is given as follows:

$$\begin{cases} x(+) = \sum_{j=1}^2 h_{\sigma(k)}^j(\rho(k))(A_{\sigma(k)}^j x(k) + B_{\sigma(k)}^j u(k) + E_{\theta, \sigma(k)}^j \theta(k)) + F_a f_a(k) + E_w w(k) \\ y(k) = Cx(k) + E_v v(k) \end{cases} \quad (66)$$

where $F_a = \begin{bmatrix} 0.0185 \\ 0.1445 \end{bmatrix}$. To illustrate actuator fault estimation capability, two different faults are considered. An abrupt fault f_{a1} and a time-varying fault f_{a2} are described as:

$$f_{a1}(k) = \begin{cases} 0 & k < 6000 \\ 0.4 & 6000 \leq k \end{cases} \quad (67)$$

$$f_{a2}(k) = \begin{cases} 0 & k < 5000 \\ 0.6 \cdot \sin(0.001\pi k) & 5000 \leq k \leq 9000 \\ 0 & 9000 \leq k \end{cases} \quad (68)$$

In order to implement the fault estimation process, an augmented SLPV system is generated as (43), where augmented matrices are designed as (44). Since T , N and \bar{C} satisfy the rank condition (48), by choosing the arbitrary matrix S as:

$$S = \begin{bmatrix} 0.1 & 0 & 0 & 0 \\ 0 & 0.1 & 0 & 0 \\ 0 & 0 & 0.1 & 0 \end{bmatrix},$$

the matrices T and N are solved using (49) as:

$$T = \begin{bmatrix} 1 & -0.0013 & 0.0183 \\ 0 & 0.5443 & 0.0787 \\ 0 & -0.0644 & 0.9907 \end{bmatrix}, \quad N = \begin{bmatrix} 0.0013 \\ 0.4557 \\ 0.0644 \end{bmatrix}.$$

By solving the LMI optimization problem (57a–c) and selecting the scalar $\varepsilon_i = 0.97$, $\varepsilon_i = 0.945$, respectively for f_{a1} and f_{a2} , the switched polytopic correction matrices $\lambda_{\sigma(k)}^j$ and the corresponding minimum ADT $\tau_a^* = 12.69$, $\tau_a^* = 16.79$ are obtained, through (56). Then, simulation results of the actuator fault estimation and the estimation error are depicted in Figures 7 and 8. For both abrupt and time-varying actuator faults, it can be seen that the proposed method is able to estimate accurate bounds of the occurred faults.

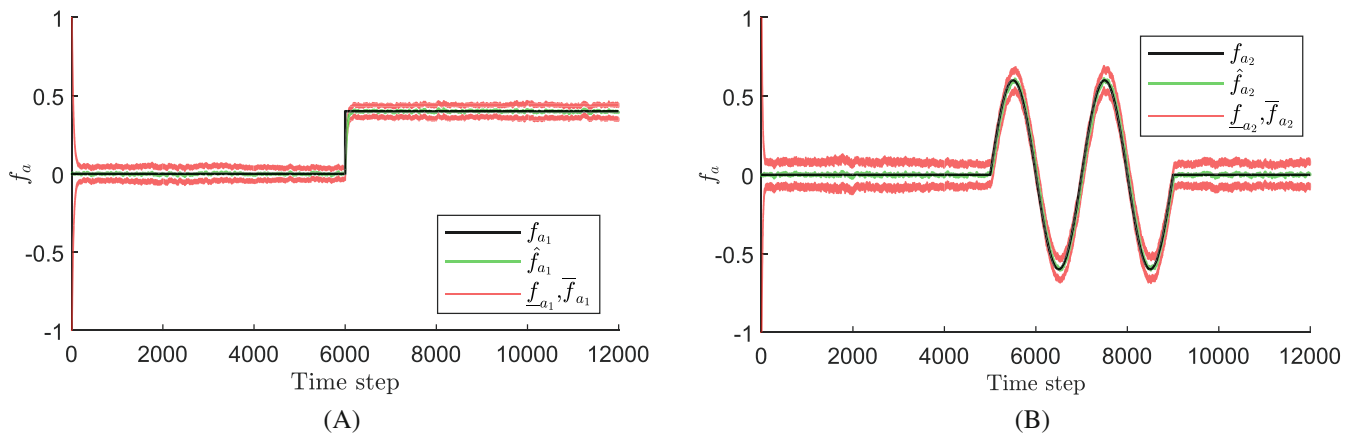


FIGURE 7 Actuator fault estimation. (A) Estimation result of f_{a1} with $\delta = 0$. (B) Estimation result of f_{a2} with $\delta = 0.002$.

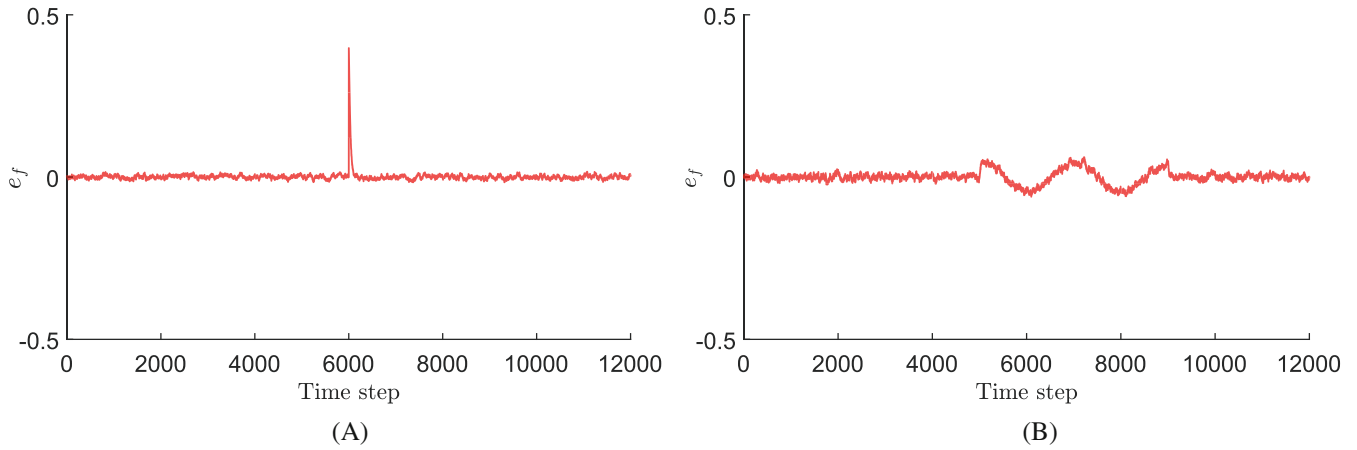


FIGURE 8 Actuator fault estimation error. (A) Estimation error of f_{a1} . (B) Estimation error of f_{a2} .

Remark 5. When estimating the time-varying faults (see Figure 7B), there is a time delay between the estimation and the actual fault. It results from the effects of fault variation. The delay phenomenon can be improved by relaxing the selection of scalar ε_i , while the relaxation leads to a wider estimated bound. Therefore, it requires a balance to guarantee both the punctual value and the estimated bound.

Furthermore, to assess the performance of the proposed method, we compare it with the Frobenius-norm (F -norm) based fault estimation method for LPV systems proposed in Reference 35. The implementation of the F -norm method is done in the case of one subsystem, that is, $\sigma(k) = 1$, if $9m.s^{-1} < v_x < 20m.s^{-1}$, where the other parameters are set the same. Then, the comparison results of fault estimation for different actuator faults are shown in Figures 9 and 10. It can be seen that these two methods provide similar estimation performance for constant fault (see Figures 9A and 10A), while the proposed method provides a more accurate punctual value estimation for time-varying fault (see Figures 9B and 10B) due to the adjustability of the proposed method as discussed in Remark 5. Furthermore, as the F -norm-based method only minimizes the intersection for each current instant, it can not guarantee the convergence of the size of the zonotopic state estimation set like the proposed method. Besides, the proposed method offers an offline way to compute the correction matrix, while the F -norm-based method computes it with a complex online computation. In this context, the proposed method is a better alternative to perform fault estimation in case of real-time applications.

6.3 | Simulation 3: Sensor fault estimation

The scenario of sensor faults is considered in this subsection, (45) is employed to generate the corresponding augmented SLPV system, with $F_s = 1$. For the simulation purpose, consider the sensor faults $f_s(k)$ described as follows:

$$f_{s_1}(k) = \begin{cases} 0 & k < 7000 \\ 1 & 7000 \leq k \end{cases}, \quad f_{s_2}(k) = \begin{cases} 0 & k < 8000 \\ 0.3\cos(0.001\pi k) & 8000 \leq k \end{cases} \quad (69)$$

From the given general solution (49), the arbitrary matrix S is chosen as:

$$S = \begin{bmatrix} 0.1 & 0 & 0 & 0 \\ 0 & 0.1 & 0 & 0 \\ 0 & 0 & 0.1 & 0 \end{bmatrix},$$

and two matrices T and N satisfying (48) are obtained and given as follows:

$$T = \begin{bmatrix} 1 & 0 & 0 \\ 0 & 0.70 & -0.30 \\ 0 & -0.30 & 0.70 \end{bmatrix}, \quad N = \begin{bmatrix} 0 \\ 0.30 \\ 0.30 \end{bmatrix}$$

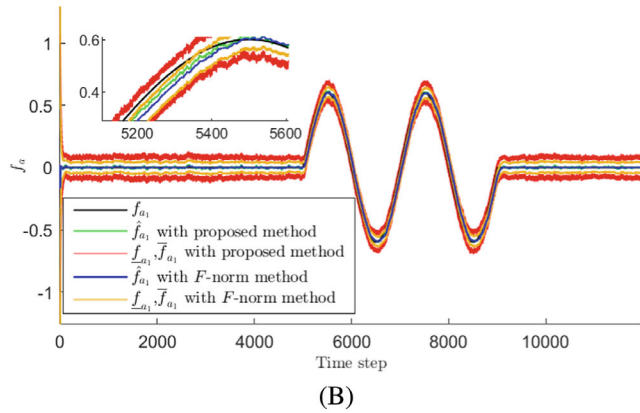
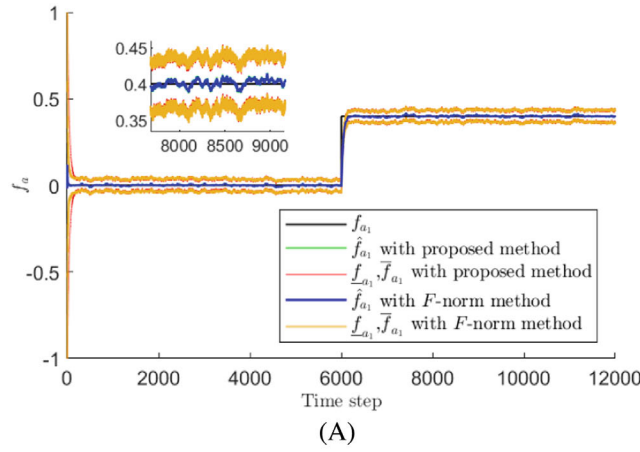


FIGURE 9 Comparison of actuator fault estimation. (A) Estimation result of f_{a1} . (B) Estimation result of f_{a2} .

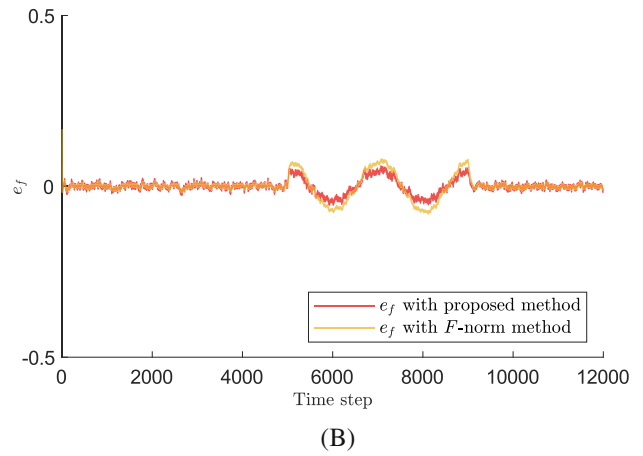
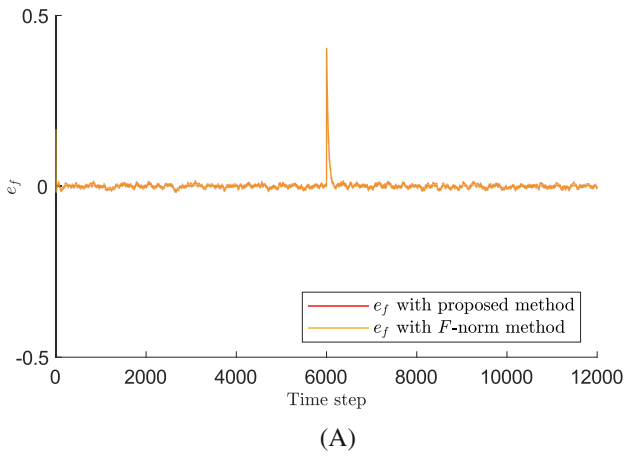


FIGURE 10 Comparison of actuator fault estimation error. (A) Estimation error of f_{a1} . (B) Estimation error of f_{a2} .

By solving the LMI optimization problem (57a–c) and selecting the scalar $\epsilon_i = 0.99$, the switched polytopic correction matrices $\lambda_{\sigma(k)}^j$ and the corresponding minimum ADT $\tau_a^* = 11.1559$ through (56) are obtained. Then, the simulation results of the sensor faults estimation are depicted in Figures 11 and 12. It can be seen that the proposed method is effective for different time-varying sensor faults and the estimated results provide satisfactory performance, including the punctual value and the upper/lower bounds.

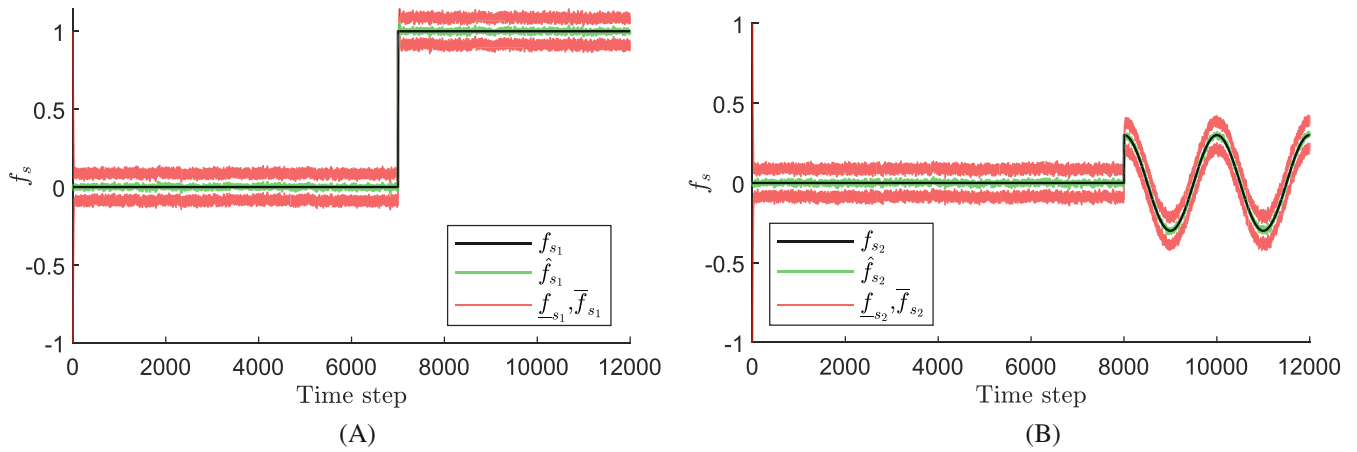


FIGURE 11 Sensor fault estimation. (A) Estimation result of f_{s1} . (B) Estimation result of f_{s2} .

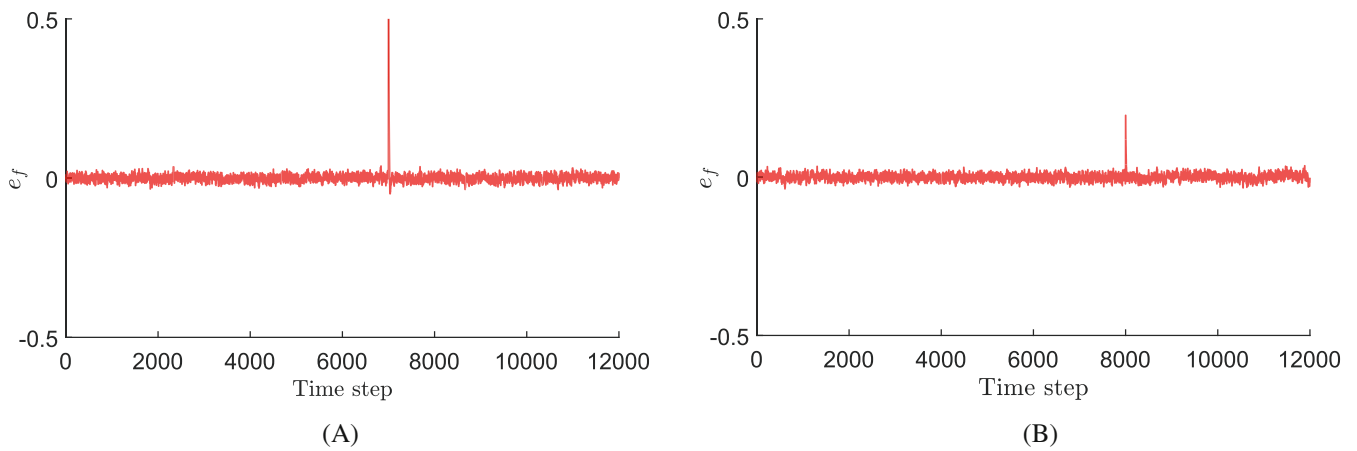


FIGURE 12 Sensor fault estimation error. (A) Estimation error of f_{s1} . (B) Estimation error of f_{s2} .

7 | CONCLUSION

In this paper, a set-membership state estimation method for SLPV systems subject to unknown but bounded parametric uncertainties, disturbances and noises is proposed using zonotopes. To guarantee a convergent and bounded estimation result, the optimal correction matrix has been designed using P -radius and ADT-based conditions, formulated as an LMI problem. With the less conservative conditions, the size of the state estimation bounds is smaller than the conventional existing results. Besides, an extension of the proposed estimation method to fault/disturbance estimation is presented. This extension allows to deal with actuator/sensor faults or input disturbances, by regarding them as an auxiliary state. Finally, the proposed method has been tested in simulation using vehicle lateral dynamics. From the state estimation simulation and comparison results, it was revealed that the proposed method is more accurate and competitive. Regarding the extension for actuator/sensor faults estimation, the simulation results have shown the effectiveness of the proposed method in the case of different types of faults. As future works, authors plan to apply the proposed state and fault estimation method for Fault Tolerant Control design of SLPV systems with ground vehicles applications.

ACKNOWLEDGMENT

This work has been co-financed by the Spanish State Research Agency (AEI) and the European Regional Development Fund (ERFD) through the project SaCoAV (ref. MINECO PID2020-114244RB-I00), by—the European Regional

Development Fund of the European Union in the framework of the ERDF Operational Program of Catalonia 2014–2020 (ref. 001-P-001643 Looming Factory), by the DGR of Generalitat de Catalunya (SAC group ref. 2017/SGR/482) and by the Chinese Scholarship Council (CSC) under grant (202006120006).

DATA AVAILABILITY STATEMENT

The data that support the findings of this study are available from the corresponding author upon reasonable request.

ORCID

Shuang Zhang  <https://orcid.org/0000-0003-4528-3326>

Vicenç Puig  <https://orcid.org/0000-0002-6364-6429>

REFERENCES

- Ping X, Yang S, Ding B, Raissi T, Li Z. Observer-based output feedback robust MPC via zonotopic set-membership state estimation for LPV systems with bounded disturbances and noises. *J Franklin Inst.* 2020;357(11):7368-7398.
- San-Miguel A, Puig V, Alenyà G. Disturbance observer-based LPV feedback control of a N-DoF robotic manipulator including compliance through gain shifting. *Control Eng Pract.* 2021;115:104887.
- Qiao D, Wang Y. Fault-tolerant control for linear parameter varying systems with integral measurements based on event-triggered mechanism. *J Franklin Inst.* 2021;358(16):8250-8269.
- Pan Z, Luan X, Liu F. Confidence set-membership state estimation for LPV systems with inexact scheduling variables. *ISA Trans.* 2022;122:38-48.
- Yang D, Zong G, Karimi HR. H_∞ refined Antidisturbance control of switched LPV systems with application to aero-engine. *IEEE Trans Ind Electron.* 2019;67(4):3180-3190.
- Lv J, Wang YE, Wu D. Observer-based control for continuous-time switched linear parameter-varying systems. *Circuits Syst Signal Process.* 2023;42(4):2049-2064.
- Zammali C, Van Gorp J, Ping X, Raissi T. Interval estimation for discrete-time LPV switched systems. Paper presented at: 2019 IEEE 58th Conference on Decision and Control (CDC). IEEE. 2019 2479–2484.
- Zhu Y, Zheng WX. An integrated design approach for fault-tolerant control of switched LPV systems with actuator faults. *IEEE Trans Syst Man Cybern: Syst.* 2022;53(2):908-921.
- Zong G, Yang D, Lam J, Song X. Fault-tolerant control of switched LPV systems: a bumpless transfer approach. *IEEE/ASME Trans Mechatron.* 2021;27(3):1436-1446.
- Shorten R, Narendra K. On the stability and existence of common Lyapunov functions for stable linear switching systems. Proceedings of the 37th IEEE Conference on Decision and Control (Cat. No. 98CH36171). IEEE. 1998 3723–3724.
- Hespanha JP, Morse AS. Stability of switched systems with average dwell-time. Proceedings of the 38th IEEE Conference on Decision and Control (Cat. No. 99CH36304). IEEE. 1999 2655–2660.
- Ifqir S, Dalil I, Naïma AO, Saïd M. Adaptive threshold generation for vehicle fault detection using switched T–S interval observers. *IEEE Trans Ind Electron.* 2019;67(6):5030-5040.
- Ethabet H, Rabehi D, Efimov D, Raissi T. Interval estimation for continuous-time switched linear systems. *Automatica.* 2018;90:230-238.
- Ifqir S, Ichalal D, Oufroukh NA, Mammari S. Robust interval observer for switched systems with unknown inputs: application to vehicle dynamics estimation. *Eur J Control.* 2018;44:3-14.
- Du D, Yang Y, Zhao H, Tan Y. Robust fault diagnosis observer design for uncertain switched systems. *Int J Control Autom Syst.* 2020;18:3159-3166.
- Li C, Zhu F, Guo S. Interval estimation and fault detection for switched nonlinear systems based on zonotope method. *Asian J Control.* 2023;25(2):1420-1431.
- Puig V, Quevedo J, Escobet T, Stancu A. Robust fault detection using linear interval observers. *IFAC Proc Vol.* 2003;36(5):579-584.
- Alamo T, Bravo JM, Camacho EF. Guaranteed state estimation by zonotopes. *Automatica.* 2005;41(6):1035-1043.
- Blesa J, Puig V, Saludes J. Robust fault detection using polytope-based set-membership consistency test. *IET Control Theory Appl.* 2012;6(12):1767-1777.
- Zhang W, Wang Z, Raissi T, Su R. An ellipsoid-based framework for fault estimation and remaining useful life prognosis. *Int J Robust Nonlinear Control.* 2023;32(12):7260-7281.
- Wang J, Lv X, Meng Z, Puig V. An integrated design method for active fault diagnosis and control. *Int J Robust Nonlinear Control.* 2023;33(10):5583-5603.
- Yang X, Scott JK. A comparison of zonotope order reduction techniques. *Automatica.* 2018;95:378-384.
- Althoff M, Frehse G, Girard A. Set propagation techniques for reachability analysis. *Ann Rev Control Robot Autonom Syst.* 2021;4:369-395.
- Kühn W. Rigorously computed orbits of dynamical systems without the wrapping effect. *Comput Secur.* 1998;61:47-67.
- Rego BS, Raffo GV, Scott JK, Raimondo DM. Guaranteed methods based on constrained zonotopes for set-valued state estimation of nonlinear discrete-time systems. *Automatica.* 2020;111:108614.
- Puig V. Fault diagnosis and fault tolerant control using set-membership approaches: Application to real case studies. *Int J Appl Math Comput Sci.* 2010;20(4):619-635.

27. Pourasghar M, Puig V, Ocampo-Martinez C. Interval observer versus set-membership approaches for fault detection in uncertain systems using zonotopes. *Int J Robust Nonlinear Control*. 2019;29(10):2819-2843.
28. Fei Z, Yang L, Sun XM, Ren S. Zonotopic set-membership state estimation for switched systems with restricted switching. *IEEE Trans Automat Contr*. 2022;67(11):6127-6134.
29. Ifqir S, Vicenç P, Dalil I, Naima AO, Saïd M. Zonotopic set-membership state estimation for switched systems. *J Franklin Inst*. 2022;359(16):9241-9270.
30. Ríos H, Mincarelli D, Efimov D, Perruquetti W, Davila J. Continuous and discrete state estimation for switched LPV systems using parameter identification. *Automatica*. 2015;62:139-147.
31. Rotondo D, Reppa V, Puig V, Nejjari F. Adaptive observer for switching linear parameter-varying (LPV) systems. *IFAC Proc Vol*. 2014;47(3):1471-1476.
32. Rotondo D, Witczak M, Puig V, Nejjari F, Pazera M. Robust unknown input observer for state and fault estimation in discrete-time Takagi–Sugeno systems. *Int J Syst Sci*. 2016;47(14):3409-3424.
33. Wang Z, Rodrigues M, Theilliol D, Shen Y. Actuator fault estimation observer design for discrete-time linear parameter-varying descriptor systems. *Int J Adapt Control Signal Process*. 2015;29(2):242-258.
34. Lan J, Patton RJ. A new strategy for integration of fault estimation within fault-tolerant control. *Automatica*. 2016;69:48-59.
35. Zhou M, Cao Z, Zhou M, Wang J, Wang Z. Zonotopic fault estimation for discrete-time LPV systems with bounded parametric uncertainty. *IEEE Trans Intell Transp Syst*. 2019;21(2):690-700.
36. Liu X, Gao Z, Chen MZ. Takagi–Sugeno fuzzy model based fault estimation and signal compensation with application to wind turbines. *IEEE Trans Ind Electron*. 2017;64(7):5678-5689.
37. Pazera M, Witczak M, Kukurowski N, Buciakowski M. Towards simultaneous actuator and sensor faults estimation for a class of takagi-sugeno fuzzy systems: a twin-rotor system application. *Sensors*. 2020;20(12):3486.
38. Le VTH, Stoica C, Alamo T, Camacho EF, Dumur D. *Zonotopes: from Guaranteed State-Estimation to Control*. John Wiley & Sons; 2013.
39. Zhang L, Shi P. Stability, l_2 -gain and asynchronous H_∞ control of discrete-time switched systems with average dwell time. *IEEE Trans Automat Contr*. 2009;54(9):2192-2199.
40. Guerra P, Puig V, Witczak M. Robust fault detection with unknown-input interval observers using zonotopes. *IFAC Proc Vol*. 2008;41(2):5557-5562.
41. Le VTH, Stoica C, Alamo T, Camacho EF, Dumur D. Zonotopic guaranteed state estimation for uncertain systems. *Automatica*. 2013;49(11):3418-3424.
42. Combastel C. Zonotopes and Kalman observers: gain optimality under distinct uncertainty paradigms and robust convergence. *Automatica*. 2015;55:265-273.
43. Penrose R. A generalized inverse for matrices. *Mathematical Proceedings of the Cambridge Philosophical Society*. Cambridge University Press. 1955 406–413.
44. Liberzon D. *Switching in Systems and Control*. Vol 190. Springer; 2003.
45. Chen J, Patton RJ. *Robust Model-Based Fault Diagnosis for Dynamic Systems*. Vol 3. Springer Science & Business Media; 2012.
46. Duan GR. *Analysis and Design of Descriptor Linear Systems*. Vol 23. Springer Science & Business Media; 2010.

How to cite this article: Zhang S, Puig V, Ifqir S. Set-membership estimation of switched LPV systems: Application to fault/disturbance estimation. *Int J Robust Nonlinear Control*. 2024;1-23. doi: 10.1002/rnc.7208